frontiers | Frontiers in Astronomy and Space Sciences

TYPE Original Research
PUBLISHED 24 October 2025
DOI 10.3389/fspas.2025.1666811

OPEN ACCESS

EDITED BY
Alberto Fairén,
CSIC-INTA, Spain

REVIEWED BY
Francesco Salese,
G.d'Annunzio University of Chieti and Pescara, Italy
Benjamin Cardenas,
The Pennsylvania State University, United States

*CORRESPONDENCE
Rebecca M. E. Williams,
williams@psi.edu

RECEIVED 15 July 2025
ACCEPTED 22 September 2025
PUBLISHED 24 October 2025

CITATION
Williams RME, Irwin RP III, Berman DC and Hill J (2025) Parallels between subaqueous ridges on Earth and Mars: a new morphological potential indicator for paleolake assessment.
Front. Astron. Space Sci. 12:1666811.
doi: 10.3389/fspas.2025.1666811

Parallels between subaqueous ridges on Earth and Mars: a new morphological potential indicator for paleolake assessment

Rebecca M. E. Williams[1]*, Rossman P. Irwin III[2], Daniel C. Berman[1] and Jonathon Hill[3]

[1]Planetary Science Institute, Tucson, AZ, United States, [2]Center for Earth and Planetary Studies, Smithsonian Institution, Washington, DC, United States, [3]School of Earth and Space Exploration, Arizona State University, Tempe, AZ, United States

Water levels in large lakes fluctuate in response to climatic cycles. Surface observations from rovers have validated past lakes on Mars, following multiple studies that inventoried candidate paleolake sites across the planet in satellite observations. Attempts to identify martian paleolake highstands, a key metric for constructing lake hydrographs, are hampered by few morphological indicators of water level discernible in orbital data. Construction of paleolake hydrographs, particularly in post-Noachian sites with preserved sedimentary deposits, holds tremendous promise for elucidating climate evolution on Mars. We examined image and elevation data at three topographic basins with established or candidate paleolakes. Drawing upon a terrestrial analog, we demonstrate that some depositional paleochannel ridges on Mars may have formed subaqueously in lakes. This new insight paves the way for future studies to use this landform in detailed lake hydrograph reconstructions.

KEYWORDS

Mars morphology, lakes, valley networks, inverted channels, surface processes

1 Introduction

Despite decades of investigation, the climatic history of Mars is only broadly characterized: (1) an early wetter period, with slow degradation and loss of impact craters, generally thought to be confined to the Noachian Period and Early Hesperian Epoch; (2) development of valley networks and paleolakes around the Noachian/Hesperian boundary; and (3) an uncertain transition to the cold, hyperarid desert present today with occasional intervals of later fluvial activity (e.g., Sagan et al., 1973; Hartmann, 2005; Howard et al., 2005; Carr and Head, 2010 Grant and Wilson, 2011). As lakes (particularly endorheic or closed-basin lakes) are sensitive to climate variations (e.g., Bradley, 2015), current research seeks to use the paleolacustrine record to constrain environmental change on Mars (e.g., Stucky de Quay et al., 2021). Although hundreds of former lake sites have been identified across the planet (Fassett and Head, 2008; Goudge et al., 2012; 2015), questions persist about the duration of standing water, a key constraint on climate conditions.

Most paleolake sites on Mars are identified by converging valley networks into a topographic basin, commonly an impact crater (Cabrol and Grin, 1999;

Fassett and Head, 2008; Goudge et al., 2012; 2015). Roughly half of the crater lake sites have an outlet valley that defines the maximum lake level at the time of the rim breach (Fassett and Head, 2008). Few crater lakes (<25%) have triangular shaped deposits, of either alluvial fan or deltaic origin, at the terminus of their inlet valley, limiting the cases where lake level is constrained from candidate deltaic deposits (e.g., Schon et al., 2012; Palucis et al., 2016). The morphological signatures of lake level changes are scarce (Irwin and Zimbelman, 2012), a fact that may be partially attributable to the extensive erosion on Mars over eons (e.g., Malin and Edgett, 2001; Edgett et al., 2020) that would remove subtle slope breaks associated with wave-cut shorelines as recently modeled by Baran and Cardenas (2025). Thus, there are few locations on Mars where lake level fluctuations can be determined and used for paleoclimate reconstruction.

In this paper, we highlight a terrestrial example of paleochannel ridges that we interpret to have been deposited subaqueously and are associated with paleolake level. The morphologic and sedimentologic attributes of paleochannel ridges at the Lake Coyote basin in southern California are described. Building upon this example, we assess the premise that some paleochannel ridge forms on Mars may mark lake level. We explore this idea through two case studies at Phison Patera and Harris crater.

2 Background: Paleolakes and paleoclimate

Lake fluctuations preserved in the terrestrial geologic records of enclosed basins are a paleoclimate indicator (Benson and Paillet, 1989; Menking et al., 2004; Godsey et al., 2005). For over a century, geomorphic characterization of lacustrine shorelines in the western United States served as the initial approach to paleoclimate reconstruction. Two foundational works focused on the largest two intermontane paleolakes, Lake Bonneville (e.g., Gilbert, 1890) and Lake Lahotan (Russell, 1885). Mapping shoreline movements over time establishes lake hydrographs, and by association, insight into relatively wet *versus* dry periods (e.g., Morrison, 1991; Reheis, 1999). These studies in the American west are representative of geomorphic climate studies conducted elsewhere on Earth (e.g., Placzek et al., 2006; Holmes and Hoelzmann, 2017; Yang and Scuderi, 2017; Fan et al., 2011, and references therein).

On Mars, former paleolacustrine sites are identified by locations where valley networks terminate or breach topographic basins. The majority of Noachian-aged (>3.7 Ga) terrain is dissected by valley networks (Carr, 1995), indicating that climatic conditions sustained surface water for periods of time around the Noachian/Hesperian boundary. Although both valley networks (e.g., Mars Channel Working Group, 1983; Carr, 1996) and candidate crater lakes (e.g., Newsom, 1996; Cabrol and Grin, 1999) were identified in Viking images, our understanding of the aqueous history on Mars has greatly expanded with geomorphic investigations utilizing high-resolution image and topographic data over the last ~25 years.

Paleolakes are classified by valley network drainage patterns, with open-basin lakes characterized by an outlet valley (Fasset and Head, 2008), and closed-basin lakes exhibiting no evidence of an outlet (Goudge et al., 2012; 2015). Over 400 candidate crater lake sites are identified: 210 open-basin lakes catalogued in Fassett and Head (2008), and 205 closed lake basins (55 of which have fan deposits) as reported in Goudge et al. (2015). [These martian crater lake catalogs generally do not consider commonplace paleochannel ridges, often called 'inverted channels,' that are the erosional remnants of channel and deltaic landforms on Mars (Malin and Edgett, 2003; Cardenas et al., 2018; Davis et al., 2016; 2019; Dickson et al., 2021)]. Some open crater lakes are linked, forming contiguous crater lake chains mainly on long regional slopes and especially in Arabia Terra, but these have subtle morphological expression and are likely under-recognized (e.g., Fassett and Head, 2008; Davis et al., 2019; Dickeson et al., 2022). This observation, that the known martian paleolake inventory may be incomplete, is one of the main research drivers for the present investigation.

In a global survey of martian fan deposits (Wilson et al., 2021; Morgan et al., 2022), putative deltas were classified based on a distal escarpment that may or may not have exposed stratigraphy, although later deflation of fine-grained deposits from the basin floor could yield a similar result (Irwin et al., 2005). Fan-deltas, landforms with both subaerial and subaqueous deposition, are difficult to identify in orbital images as this discrimination is based on sedimentologic attributes (e.g., steeply dipping foresets). Few fan deposits on Mars have exposed bedding stratigraphy to reinforce classification as lacustrine delta deposits in orbital images (e.g., Malin and Edgett, 2003; Moore et al., 2003; Irwin et al., 2015; Goudge et al., 2017; Fawdon et al., 2018).

Constraining the time sequence of martain lakes is hampered by limited morphological evidence. Geomorphic investigations have identified former lake levels and determined evolutionary sequences in only a few martian lacustrine basins (e.g., Palucis et al., 2016). Several of these studies are associated with proposed landing sites for Mars missions: the deltaic complex in Eberswalde crater (e.g., Malin and Edgett, 2003; Moore et al., 2003; Irwin et al., 2015), at least two lake episodes in Holden crater (Grant et al., 2010), and the fan complex in southwest Melas basin (Williams and Weitz, 2014; Davis et al., 2018). *In situ* rover investigations at two paleolacustrine sites have confirmed that standing water was present at Gale crater (Grotzinger et al., 2015) and the Jezero crater (Mangold et al., 2024). Observations from the *Curiosity* and *Perseverance* rovers led to formulation of detailed lake histories (Schieber et al., 2020; Schieber et al., 2024; Caravaca, 2024; Williams et al., 2023).

3 Materials and methods

We used image and topographic data to characterize paleochannels at basins with known or possible paleolacustrine history: one field site (Lake Coyote, California) and two Mars sites (Phison Patera and Harris crater).

A note on nomenclature: In this paper, we will use paleochannel or paleochannel ridge to indicate sites where prior work has documented the former course of a fluvial system through attributes of the sedimentary deposit and/or landform character. More specific terminology for paleochannels will be used when appropriate (see Section 4.1).

3.1 Data sets for Earth: Lake Coyote, CA

Satellite data for the field site in the Californian Mojave Desert was examined on Google Earth (Google Earth, 2024). In addition, we used aerial high-resolution orthoimagery from the USGS EarthExplorer including the Digitial Orthophoto Quadrangles (DOQs) originally collected on 01 October 1995: Harvard Hill (O3411603.NWS.839561) and Alvord Mountain West (O3511659.SWS.839536). Regional meter-scale topographic data are from airborne LiDAR (Light Detection And Ranging) acquired in August 2017 (accessible at USGS Lidar Explorer https://www.usgs.gov/tools/lidarexplorer).

Field studies, measurements, and observations at the paleochannel ridges were conducted between the years 2014 and 2016. Photo documentation of paleochannel ridges included landscape views and nadir surface images for grain size statistics following methods of Bunte and Abt (2001). Topographic surveys of paleochannel ridges used the Trimble Pro XRS Differential Global Positioning System (DGPS), with 2–4 cm horizontal and vertical precision in the acquired elevation data. Elevation measurements were used to characterize ridge shape with spot points acquired along longitudinal and cross-sectional ridge transects.

3.2 Data sets for Mars: Phison Patera and Harris crater

Images used in this study are from two cameras on board the Mars Reconnaissance Orbiter: the High Resolution Imaging Science Experiment (HiRISE; 0.25 m/pix; McEwen et al., 2007) and the ConTeXt camera (CTX, ~6 m/pix; Malin et al., 2007) rendered into a global mosaic (Dickson et al., 2024; available online through the Caltech Murray Lab; https://murray-lab.caltech.edu/CTX).

We also examined multipsectral Thermal Emission Imaging System (THEMIS) infrared images (Christensen et al., 2001). Decorrelation stretched (DCS) images are produced from THEMIS band 9 (center wavelength 12.57 μm), band 6 (10.21 μm) and band 3 (7.93 μm) mapped to red, green and blue, respectively. These data are advantageous because they illustrate the maximum spectral variability within THEMIS data in a 3-band set. THEMIS DCS-963 quadrangles are generated according to the procedures described in Hill (2022) to have globally consistent colors. These data are currently available to the THEMIS science team for validation prior to archival for the planetary science community.

Topographic data are from the Mars Global Surveyor Mars Orbiter Laser Altimeter (MOLA, Zuber et al., 1992) blended with High-Resolution Stereo Camera (HRSC; Neukum et al., 2004) digital elevation models (DEM, 200 m/pix resolution, ~10 m vertical precision; Fergason et al., 2018; Gwinner, 2010; Kirk et al., 2021). Where available, we generated high-resolution CTX-DEMs (24 m/pix resolution, ~5 m vertical precision Kirk et al., 2021) using the Ames Stereo Pipeline (Beyer et al., 2018; Mayer and Kite, 2016; Mayer, 2018). Data products produced during this study are archived with the USGS Science Base (Williams et al., 2024).

Geomorphic features mapped in previous studies were also incorporated into the JMARS (Christensen et al., 2009) GIS database. We used the global map of valley networks (Hynek, 2016). Davis et al. (2019) mapped sinuous ridges, interpreted as inverted channels, in Arabia Terra. In a regional study of the northern Hellas basin, Gullikson et al. (2023) mapped fan deposits and catchments, valley networks, ridges, fan deposits and catchments.

FIGURE 1
Schematic to illustrate our approach to qualitatively evaluate martian paleolakes in this study.

3.3 Assessing subaqueous ridge origin within two martian basins

We selected two case study locations on Mars with paleochannel ridges within closed topographic basins: northern Arabia Terra and Harris crater. These sites were selected because they have not previously received detailed consideration as lacustrine sites, and they have mapped ridges interpreted as raised channels formed through topographic inversion. Our approach is described below and the workflow is illustrated in Figure 1.

3.3.1 Correlating possible lacustrine shoreline landforms

Our primary approach is to compare the elevation of landforms that could be associated with a lake. Principally, we examined the upper elevation of paleochannel ridges—understanding that their surroundings are deflated and they may be exhumed from more than the original channel depth—and the termination elevation of valley networks.

Where there is downstream longitudinal continuity from valley networks to contiguous ridges, this elevation interval records an important transition within the system. This zone could correspond to conditions that fostered sediment deposition (i.e., slope change, lacustrine depositional setting). Another possibility is that this interval marks erosion of fluvial deposits (topographic inversion).

These elevations informed evaluation of specific candidate lake levels. The goal was to select representative elevations for past lake level for comparison with other possible indications of a paleolake (e.g., alluvial deposits that are hanging rather than graded to the basin floor, a distal slope on a deposit as a possible foreset, and topographic benches potentially resulting from wave action). More broadly, we also considered the regional setting, including the spatial association of putative paleolacustrine deposits (Figure 1).

For this consistency study assessing candidate lake levels we adopted an elevation range for coincident values of 30 m based on the horizontal resolution of images and the vertical error of the DEMs (Gwinner, 2010; Kirk et al., 2021). We considered features to be 'nearby' when they are within 90 m elevation (threefold the criteria for matching the candidate lake level) to account for the scale of mapped features (accuracy of feature extents), landform setting (e.g., nearshore, onshore, beach, *etc.*) and landform preservation. This approach is consistent with other geomorphic evaluations of lake stands on Mars with comparable datasets, for example at Gale crater (Palucis et al., 2016). We used the modern topography

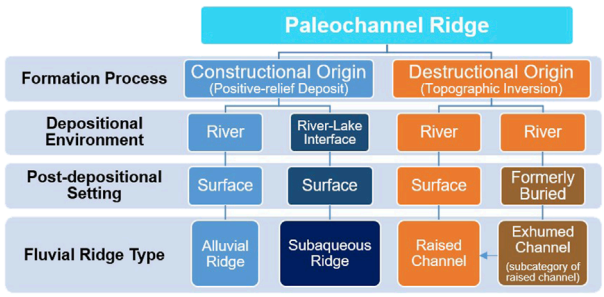

FIGURE 2
Schematic to delineate paleochannel ridge terminology used in this paper. See text description in Section 4.1.

and assume minimal post-deposition landscape modification (e.g., regional tilting, faulting, *etc.*). Due to erosion, ridges may be only partially preserved; this incomplete record would result in a lower elevation value for the upslope end and a lower concurrence with landform elevations at sites around the basin.

3.3.2 Mapping indurated crater fill

Circular features of minimal relief or elevated plateaus are common across Arabia Terra. Such features are thought to represent the eroded remnants of indurated crater fill deposits and are likely remnant paleolake deposits (Davis et al., 2019). In that study, none of these features were noted within Phison Patera. Here, we re-examined the broader Phison Patera region in northeastern Arabia Terra to map circular features that are flat or elevated. We mapped in an area bounded between 25.5° to 36.5°N latitude, and 38.5° to 62.0°E longitude. Most of these features have distinct thermal infrared spectral signatures that appear purple in the THEMIS DCS-963 mosaic. We excluded similarly colored areas in DCS-963 within craters, as well as irregularly-shaped topographically high features. Mapping was conducted at 1,024 pixels per degree. The smallest features recorded were 2 km in diameter.

4 Results: Paleochannel ridges associated with paleolakes on Earth

4.1 Background—Polygenetic paleochannel ridge formation

The former course of rivers is preserved in a number of ways. Paleochannels are the relict fluvial path identified by sedimentary deposit and/or landform attributes (e.g., planimetric network pattern; Bridge, 1984; 2003; Miall, 1985; Church, 2006; Fielding, 2007; Hooke and Yorke, 2011; Ashmore, 2013). These deposits can be single channel-fill, channel belt or alluvial-valley-fill deposits (Hayden and Lamb, 2020). Paleochannel ridges are positive-relief features whose origin may be primary (constructional deposit) or secondary (inverted-relief landform) fluvial deposits (Figure 2).

Topographic inversion in fluvial systems occurs where differential erosion removes the intervening erodible material and the relic fluvial channel fills, channel belts or valley fill material are preferentially preserved in an elevated state relative to the surrounding terrain (Maizels, 1990; Pain and Ollier, 1995; Pain et al., 2007; Hayden et al., 2019; Zaki et al., 2020; Zhao et al., 2021). Such landforms are termed raised channels, inverted valleys, the colloquial 'inverted channels' (a term that is pervasive in the martian literature), or exhumed channels when formerly buried prior to topographic inversion (Williams et al., 2007; Cuevas Martínez et al., 2010; Foix et al., 2012; Cardenas et al., 2020; Korus and Joeckel, 2023; Clarke et al., 2020; Williams et al., 2009; Williams et al., 2011). Various processes can cause fluvial deposits to become indurated, whether from cementation, armoring by coarse sediment or infilling by lava flows (Pain and Ollier, 1995; Pain et al., 2007). Subsequent erosion of the channel banks and/or floodplain results in topographic inversion, transforming the original low-lying channel deposits into an elevated ridge. A recent global inventory of over 100 raised channels on Earth documents a range of erosion-resistant capping materials (Zaki et al., 2021), but all of these landforms have a destructive origin.

Primary paleochannel ridges are well documented in the literature. Alluvial ridges are near-channel positive-relief regions associated with changing river courses due to avulsion (Fisk, 1944; Allen, 1965). As a river channel migrates over time, channel belt dynamics generate alluvial ridges through overbank deposition (Allen, 1965; Bridge and Leeder, 1979; Bridge, 1984; Nicholas et al., 2018; Slingerland and Smith, 1998). This sediment deposition is the river's store of potential energy (Gearon and Edmonds, 2025). Aggradation of the channel beds and banks of rivers form alluvial ridges. The most detailed study of alluvial ridges is from the modern Mississippi River and more broadly along the coastal plain of the northern Gulf of Mexico (Fisk, 1944; 1952; Aslan and Blum, 1999; Swartz et al., 2022), and thus the term is generally associated with fine-grained sedimentary systems. Alluvial ridges are discontinuous landforms that record abandoned river channels generated over timescales of centuries to millennia (Fisk, 1944; Blum and Price, 1988; Kiss et al., 2022).

In contrast, and of relevance to this work, a newly recognized mechanism of primary paleochannel ridge formation is subaqueous generation at the interface between a river and a rising lake (Miller et al., 2018). This is a constructional scenario, wherein the fluvial deposits are emplaced in a ridge-form at the time of deposition. Paleochannel ridge relief may be enhanced due to secondary erosional processes as the lake level falls. In the next section, we describe field observations from such a location as an illustration.

4.2 Terrestrial paleochannel ridges associated with paleoshoreline at Lake Coyote, CA

Lake Coyote is a playa (~5 km × 7 km), one of four subbasins of Pleistocene Lake Manix in southern California (Figure 3; Supplementary Figure S1). Lacustrine phases at Lake Coyote occurred at times during the last 25 ka when water in the Mojave River breached the 543 -meter-above-sea-level (masl) threshold, crossing the Minneola fluvial plain and entering the Coyote basin (Meek, 1994). During this time interval, the basin was tectonically stable (Miller et al., 2018).

Distributary paleochannel ridges above the Minneola fluvial plain were first identified by Hagar (1966). Trenches dug into

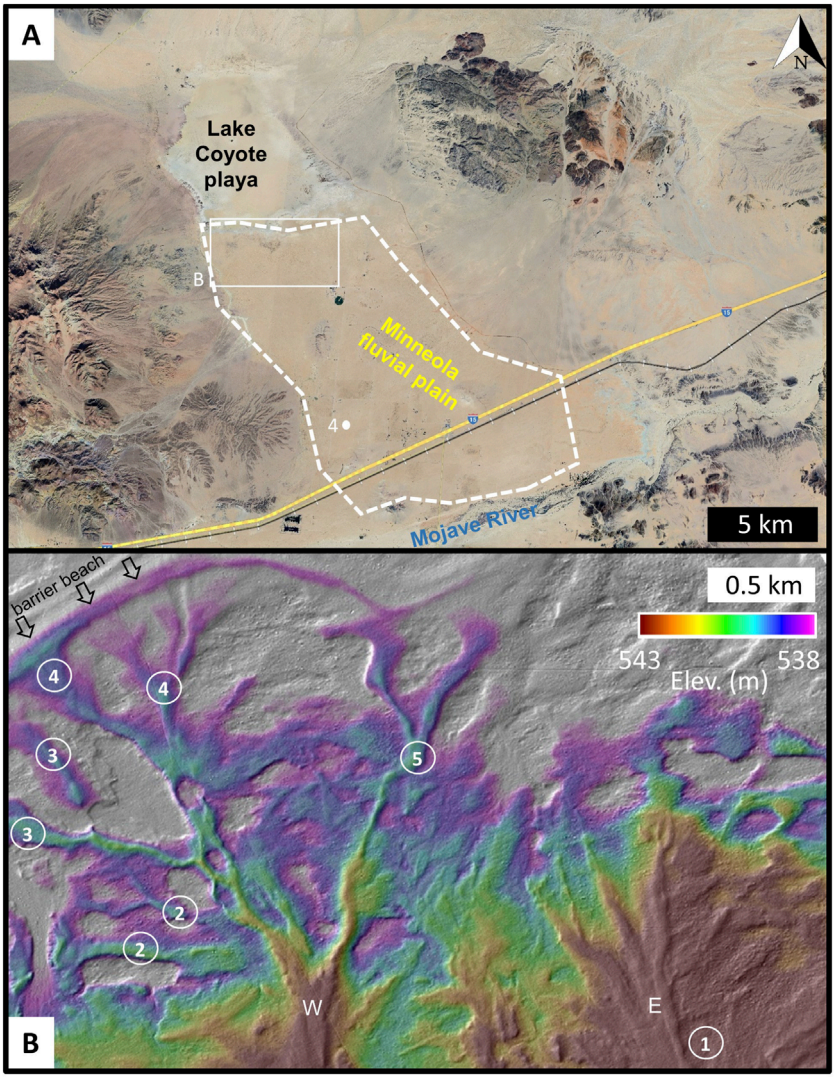

FIGURE 3
(A) Location map for inverted channels associated with Pleistocene Lake Coyote playa in southern California. Paleochannel ridges are present across the area north of Mojave River in the Minneola fluvial plain (dashed white line). White dot marks location of Figure 2. Satellite image date 11/29/2023, centered near 35°1.5′ N, 116°37.7′ W, accessed through Google Earth on 12/13/2024. **(B)** LiDAR shaded relief map with a color-ramp highlighting a 5 m elevation range to illustrate eastern and western (E, W) paleochannel ridge form. Miller et al. (2018) established a fluvial sequence (circled numbers) of inverted channels stepping basinward. See Supplementary Figure S1 for regional context.

the ridges revealed channel-fill geometry with thicker coarse sand deposits at ridge center tapering laterally to the edge and sediment composition confirmed provenance (Hagar, 1966; Dudsah, 2006). Mojave River deposits contain arkosic sand sourced from the California Transverse Ranges, and gravels of plutonic rocks and metasedimentary rocks, including distinct rounded quartzite (Miller et al., 2018). At the ridge margins, the Mojave River deposits interfinger with lacustrine silt deposits. Further, stratigraphic sections along the Lake Coyote margin show Mojave River sediments (identified by the presence of diagnostic quartzite pebbles, the bed load of the Mojave River) buried by thin lacustrine deposits (Miller et al., 2018).

The spatial configuration of the ridges is best recognized in remotely sensed data. The ridges at Lake Coyote are evident in aerial photographs by dark tone (varnished gravel) of ridges in contrast to lighter-toned plains, and minor vegetation patterns (sparser on crest). Dudsah (2006) mapped two broad paleochannel ridge systems (eastern and western). Miller et al. (2018) conducted a detailed map of individual ridges in sub-meter topographic data, documenting a direct connection to the Mojave River. The eastern set of paleochannel ridges have bulbous terminations, whereas the western set end as individual radial ridges (Figure 3B). The terminal elevation of the western paleochannel ridges merge with an arcuate barrier beach.

Mapped ridges are widespread across the Minneola fluvial plain, covering an area of ~115 km^2. These landforms vary in size (Supplementary Figure S2), with ridges ranging from 10–30 m wide, and segments extending in length from a few meters to over a kilometer. The ridges exhibit low relief, generally less than 1 m, with a very shallow northerly slope (~0.11°) along their crest (Supplementary Figure S2).

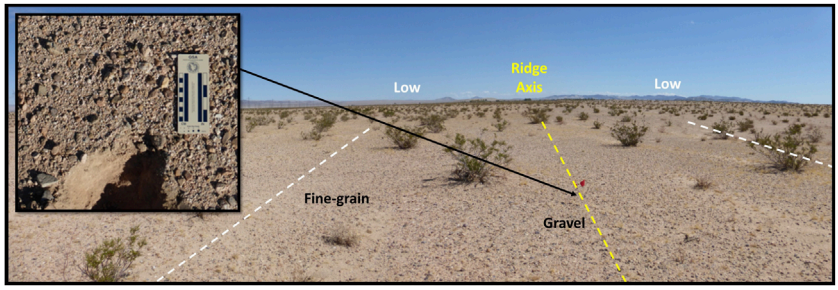

FIGURE 4
Paleochannel ridges adjacent to Lake Coyote, California, are barely discernible at the site due to low relief and minor grain size variations in the surface material. Photo along ridge axis (yellow line) shows sparse gravel concentrated on topographic high and decreasing grain size towards the lowlands. Distance between dashed white lines is ~10 m. Inset: Trench shows gravel monolayer over unconsolidated fine-grained sediment (sand to silt), inferred lacustrine deposit. Image location is marked on Figure 3A and is near 34.96071°N, 116.68867°W (9/18/24).

Due to their subtle topographic form, the ridges are difficult to recognize from surface expression in the field. A monolayer of clasts blankets the surface of the Minneola fluvial plain, with grain size varying with topography (Figure 4). Gravel is concentrated on the ridge crest, while finer-grained sediment is present in the lowlands. At the ridge apex, the maximum grain size reaches coarse gravel (2 cm), in contrast to the topographic lows where the coarsest fraction is fine gravel (0.5 cm). Correspondingly, median grain size also differed: D_{50} = 0.9 cm at the crest and D_{50} = 0.2 cm in the trough. These gravelly fluvial deposits are thin (a veneer) and superpose earlier lacustrine deposits composed of silt-to sand-size grains. In general, ridge sediments are unconsolidated sediments and weakly cemented by halite salt, making them easily excavated by hand. Locally, ridges have soil present beneath the gravel pavement that can reach 5 cm thickness and is well indurated with calcium carbonate.

4.3 Interpretation: Terrestrial paleochannel ridges associated with paleoshoreline at Lake Coyote, CA

In a preliminary United States Geological Survey (USGS) geologic map, Dudsah (2006) outlined three working hypotheses for the Lake Coyote paleochannel ridge origin with reference to analog sites: 1) differential erosion of Mojave River channel deposits (raised channels similar to the gravel-capped exhumed river channel systems in Oman; Maizels, 1990), 2) fluvial deposition in a low gradient aggrading system (potentially akin to the Australian Lake Eyre; Lang et al., 2004), or 3) a mixture of both destructive and constructive processes (e.g., a combination of hypotheses 1 and 2).

Observations support both destructive and constructional processes (favoring model 3), which highlights the complex history preserved in the Lake Coyote paleochannel ridges. Importantly, these two paleochannel ridge types are gravel-capped ridges that are indistinguishable in undisturbed surface observations. Clast armoring by river-transported gravels protected finer-grained sediment in this deflated landscape. Thus, the gravel-capped ridges are interpreted as raised channels, differentially eroded stream channel deposits, with the low-lying finer grain deposits between ridge crests interpreted as marsh and floodplain deposits (Hagar, 1966; Dudsah, 2006; Miller et al., 2018). However, at the lake margin the geomorphic and sedimentologic signature of streams interacting is consistent with constructional channel deposition (e.g., gravel-capped subaqueous ridge).

The Lake Coyote site is noteworthy for the positive-relief geomorphic expression of the stream-to-lake margin with two varieties of constructional subaqueous ridges. The eastern paleochannel ridges end very close to the maximum Lake Manix highstand (543 masl at 24.5 ka; Figure 3B), potential evidence that the river flowed into standing water (Dudsah, 2006; Miller et al., 2018). Miller et al. (2018) proposed that rivers entering the Coyote basin encountered a rapidly rising lake such that river deposits were buried by lacustrine sediments as water levels rose, a situation they suggested inhibited delta formation.

In contrast, the western paleochannel ridges are interpreted as constructional channels whose sediment was reworked to form an arcuate barrier beach. Paleochannel ridge elevation matches the barrier beach at an altitude of ~541 masl. In this area, Miller et al. (2018) documented river channel position moved progressively eastward from stratigraphic relationships of the radial ridges and confirmed by radiometric dating (Figure 3B). They propose that wave action and lake currents along the beach transported north-flowing bed load away (along shore), explaining the source of gravel sediment and overall shape of the arcuate barrier beach.

Lake cycles were initially constrained by geomorphic mapping to establish a relative sequence. *In situ* stratigraphic sections and radiometric dating of lacustrine shells were then used to establish an absolute chronology (Oviatt, 1997; Miller et al., 2018). These data allowed Miller et al. (2018) to identify six lake cycles spanning ~5 ka, with an associated fluvial sequence as the paleochannel ridges progressively stepped basinward (Figure 3B). Radiometric ages differentiate depositional phases for individual radial ridges ('spokes') at the end of the western paleochannel ridges, and the apparent distributary configuration of ridges is a time-integrated pattern. The eastern paleochannel ridges formed first, followed by sequential radial ridge accretion along the western lake margin (Figure 3B). The paleochannel ridges record a time sequence of river channel switching.

FIGURE 5
Location map of two case study sites are marked with stars. Global map with latitude extent from 50° to −55°. Image Credit: National Geographic Society/MSSS/MOLA Science Team/JPL/NASA.

Lake Coyote had a minimum fill time of 30 years based on estimated river discharge rates, but the integrated regional climate-hydrological record indicates sustained lake stands with duration of several hundred years (Wells et al., 2003; Miller et al., 2018). This highstand longevity argues against paleochannel deposits occasionally drowned by the lake, and supports the river-lake confluence model.

Lake hydrographs are often compared to other paleoclimate records to infer information on regional or global trends. Reheis et al. (2015) compared the Lake Manix hydrograph with ice core, marine and speleothem paleoclimate records. They documented three highstands for Lake Manix that coincide with known climate events (abbreviated here as Henrich events: H2, H3 and H4). Supplementary Figure S3 shows the reconstructed lake level curve for Late Pleistocene Lake Manix. The subaqueous paleochannel sequence at Lake Coyote corresponds to the most recent warming period, occurring after the H2 event.

5 Results: Assessing paleochannel ridges associated with paleolakes on Mars

Martian paleochannel ridges are commonly identified in images by planform morphology, tonal contrast and shadows cast by ridge walls, rather than by relief or cross-sectional form in topographic data (Pain et al., 2007; Williams et al., 2013; Davis et al., 2016; Dickson et al., 2021; Davis et al., 2025). They are significantly larger than the potential analog Lake Coyote landforms described here, with widths of hundreds of meters to a few kilometers. This size disparity is in part due to the limited image coverage at meter-scale or smaller resolution, inhibiting detection of comparably scaled landforms on Mars. In addition, Mars has experienced several cycles of deposition and erosion, evidenced in part by filled and excavated impact craters across the planet (e.g., Malin and Edgett, 2000; 2001; Day et al., 2016; Grotzinger et al., 2015; Edgett et al., 2020). As a result, martian paleochannels, especially smaller ones, are likely missing due to overprinting by burial or removal by erosion. These factors promote a preservation bias of larger landforms.

Using the Lake Coyote analog as a framework to consider new martian paleolake sites, we examined two closed basins with previously identified paleochannel ridges for the purposes of assessing the former presence of a lake (Figure 5; Supplementary Figure S4).

5.1 Case study 1: Phison Patera, Mars

Arabia Terra is the northern extent of the martian ancient cratered highlands and is noteworthy for the relative scarcity of valley networks compared to other Noachian-era terrains (Hynek et al., 2010). Fluvial systems in Arabia Terra were active between the mid-Noachian to Early Hesperian (Davis et al., 2018). With the recognition that some martain fluvial systems are preserved as topographic highs due to differential erosion (e.g., Dickson et al., 2021), paleochannel ridges help bridge the gaps in some valley networks and expand the record of surface runoff on Mars.

In Arabia Terra, Davis et al. (2016) mapped a contiguous pattern of fluvial landforms showing negative-relief valleys transitioning to positive-relief ridges ('inverted channels'). This morphological transition was interpreted as crossing an erosional boundary, reflecting a complex history of burial and exhumation (Davis et al., 2016; 2018).

Northeastern Arabia Terra has long been recognized as the site of an extensive mantle up to several hundred meters thick that covers the ancient Noachian cratered terrain (Moore, 1990; Fassett and Head, 2007; Zabrusky et al., 2012). The horizontally layered mantle is thought to be a regional aeolian, dust or pyroclastic deposit that has been extensively denuded to form scabby or 'etched' terrain (Edgett, 2005; Hynek and Di Achille, 2017), with an estimated original etched unit thickness of ~800 m at Phison Patera (Zabrusky et al., 2012). Davis et al. (2019) demonstrated the high correlation (~80%) of paleochannel ridges and the former extent of etched terrain in Arabia Terra. They suggested that the blanketing etched terrain may have protected the paleochannels from erosion such that the low-relief ridges visible today are the final stages of the significant deflation experienced across Arabia Terra. With this history of burial and erosion, the Phison Patera paleochannel ridges are exhumed channels.

Phison Patera is a topographic basin located in northeastern Arabia Terra, centered near 30°N, 48°E (Figure 6). [The International Astronomical Union name is for an albedo feature originally mapped by Antoniadi (1930)]. Identified as a quasi-circular depression in MOLA data by Frey et al. (2002) and dated to the Early Noachian, it is an eroded composite impact basin. As a large regional sink, valley networks incise the perimeter but lack triangular deposits at their termini. Davis et al. (2019) first proposed this site as a candidate paleolake based on transitions from valley to exhumed channels terminating within a ~400 km-diameter closed basin (~10^5 km^2). This location is not included in martian crater lake databases (Fassett and Head, 2008; Goudge et al., 2012).

To evaluate a possible paleolake at the Phison Patera basin, we considered morphological evidence for consistency with standing water at this site. First, we assessed candidate lake levels based on the transition zone between valleys and exhumed channels. Second, we examined the spatial distribution of indurated crater fill that are likely remnant paleolake deposits, as described in Section 3.3.2.

5.1.1 Fluvial morphological transition

Seven fluvial systems terminate within the Phison Patera basin. These systems are characterized by an inlet valley network that connects downslope with a curvilinear ridge, interpreted as a paleochannel subjected to topographic inversion (Davis et al., 2019).

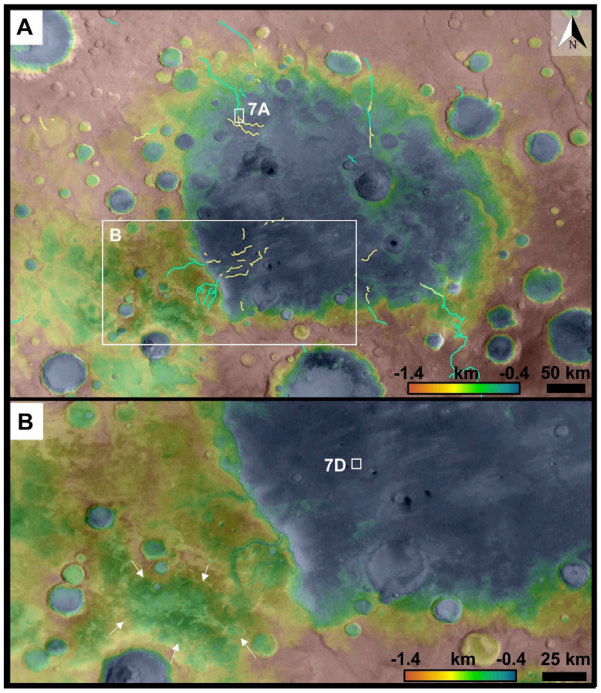

FIGURE 6
(A) Context map of Phison Patera is shown in blended MOLA/HRSC DEM (Fergason et al., 2018) overlain on CTX basemap centered at 30.0°N, 47.5°E. Lines are mapped valley networks (cyan) from Hynek (2016) and ridges interpreted as paleochannel ridges (yellow lines) from Davis et al. (2019). **(B)** Subscene enlargement to illustrate shallow lowlands (arrows) at heads of valley networks entering the basin from the southwest.

The exhumed channels maintain the full breadth of their feeder valley (widths of 1–2 km) at the transition and extend several tens of kilometers into the basin (Figure 7). Paleochannel ridge planform ranges from straight to modestly sinuous, with some cases splitting downslope (Figures 7A,C). Ridge width is relatively consistent along course and is typically a few hundred meters. Boulders are observed on the ridge surfaces (Figures 7B,E). The cross-sectional shape of the ridges appears to be flat-topped, and the ridge relief appears modest (Figure 7C).

Supplementary Table S1 reports the elevation range between the termination point of the mapped valley network (Hynek, 2016) and the onset elevation of the paleochannel ridge aligned with that valley (mapped by Davis et al., 2019). In cases where the features mapped by these researcher overlap, that elevation range was recorded. The elevation interval between these landforms may record lake highstands.

Two candidate lake levels were identified through this exercise with matching elevations (<30 m; Supplementary Figure S5). (Broadening the elevation range to <90 m did not add locations.) Four fluvial systems had overlapping elevation ranges with matching values for the paleochannel ridges. A representative candidate lake level of −1,300 m for this group is illustrated in Figure 8A and Supplementary Figure S6, covering an area of ~80,000 km^2. A higher candidate lake level at −900 m (Figure 8B) coincides with two other fluvial systems in the southern portion of the basin. This candidate lake level covers an area of ~135,000 km^2. One fluvial system, #5, had an elevation range for the valley-to-ridge transition at approximately −750 m, which could represent the maximum lake level.

5.1.2 Paleolake morphology

Indurated crater fill was mapped regionally in the area surrounding Phison Patera (bounds 24.5°–36.5°N; 38.5° to 62.0°E). Note that Davis et al. (2019) did not mark any indurated crater fill at this location, although they did note occurrences throughout Arabia Terra (see their Figures 1, 6). This difference may be due to the subtle expression of these features in visible-wavelength images (e.g., HiRISE, CTX), as there is minimal tonal difference relative to the surrounding terrain. However, the thermal and spectral signature of indurated crater fill permits rapid identification of these distinct rounded landforms in the THEMIS DCS-963 mosaic (Figure 9).

Eighty-eight indurated crater fill features were identified (Supplementary Table S2). A subset of the mapped area is illustrated in Figure 9B to show the spatial association of features within the proposed Phison Patera paleolake site. Thirty-four mapped indurated crater fill features are clustered together, and very few (n = 4) are located on the adjacent terrain outside of the basin (Figure 9).

5.1.3 Interpretation: Phison Patera, Mars

The case for a hypothesized lake at Phison Patera is strengthened by the commonality of valley network to ridge transitions associated with two evaluated highstand elevations (Figure 8; Supplementary Figure S5). We interpret the continuity of the valley network to paleochannel ridge transition as a contemporaneously formed system responding to lake level, rather than marking an erosional boundary as previously suggested. The strongest case is for a lake level at −1,300 m, with four fluvial systems spanning at least half the basin circumference meeting the elevation criteria. The close elevation agreement in ridge onset despite the range in distance from the basin edge (referenced to −900 m; Figure 8B) is suggestive of a river encountering a lake, and a more likely explanation than aeolian erosion coinciding with an elevation contour. Reinforcing this interpretation is the concentration of indurated crater fill within this topographic basin (Figure 9) that is likely remnant paleolake deposits similar to those identified in the vicinity by Davis et al. (2019). Together, these morphological landforms are consistent with a paleolake (Table 1). Evidence for the maximum lake level (−900 m) is limited (only two matches), and we categorized it as plausible to convey that a high lake is possible but not well recorded in the landscape.

The Phison Patera paleolake ranks in the top 5% of martian crater lakes by area (Goudge et al., 2015) and broadens the extent of widespread aqueous systems across Arabia Terra. It is comparable in size to the largest paleolakes in the region (e.g., Cassini, Tikhonravov, and Antoniadi craters; Fassett and Head, 2008). Additionally, the Phison Patera basin is located immediately northeast of the longest crater lake chain system identified to date on Mars: the Naktong-Scamander-Mamers (NSM) system extends ~5,000 km in length and has a ~2.4 × 10^6 km^2 catchment (Irwin et al., 2005; Fassett and Head, 2008; Davis et al., 2019). The Phison Patera area differs from the integrated NSM system as it is rimmed by relatively short, single-thread valleys that apparently drained shallow lowlands (Figure 6B). A regional groundwater

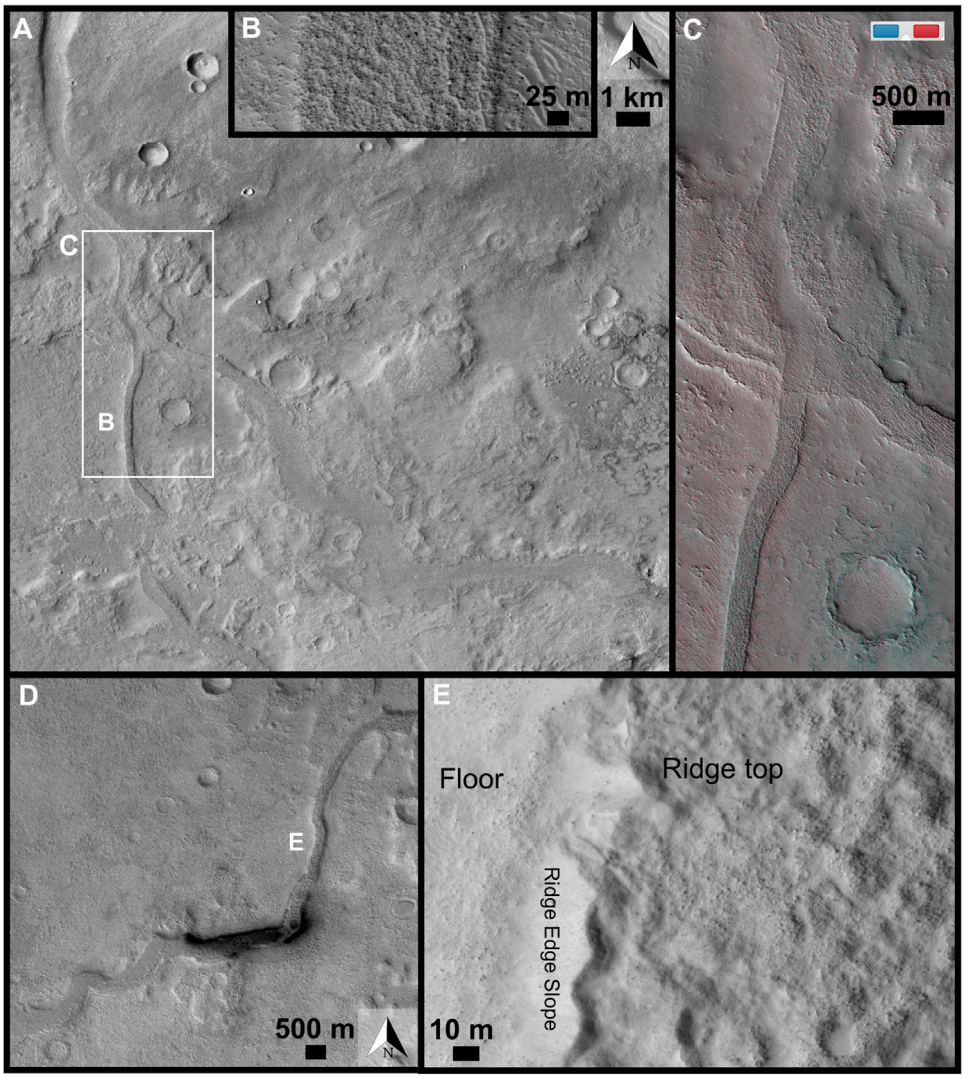

FIGURE 7
Examples of ridges in Phison Patera. **(A)** Subscene of CTX mosaic illustrating valley network to paleochannel ridge transition. Location is basinward from #1 in Figure 8A, near 32.21°N, 45.99°E. **(B)** High resolution subscene showing boulders on ridge surface. **(**HiRISE PSP_005355_2125). **(C)** Anaglyph subscene to show modest ridge relief (estimated <10 m). (HiRISE PSP_005355_2125 and ESP_084304_2125. Image credit: NASA/JPL-Caltech/UArizona). **(D)** Sinuosity of ridge varies along course in this example located basinward from #3 in Figure 8A. Subscene of CTX mosaic near 28.95°N, 46.18°E. **(E)** High resolution subscene showing boulders on ridge surface. (HiRISE ESP_037674_2090). Illumination is from the upper left in all panels.

system, as inferred for this area by Fassett and Head (2008), was likely a source of water to lakes especially in the lower elevations and for deep craters with few inlet valleys.

The geologic setting is consistent with finite periods of regional flooding. Single-stem to anabranching valleys incise into the terrain and mantle (Figure 6), and locally divert around the ejecta blanket of young impact craters. The highly erodible mantle (etched unit) is inferred to be fine-grained, possibly dust-size (Moore, 1990), and would be readily subjected to aeolian deflation as well as transported in flows as suspended load. Mapped paleochannel ridges extend well into the basin center (e.g., #3 and #4 in Figure 8A), an indication of the high energy transport capacity.

We speculate that the paleochannel ridges here are constructional in nature, possibly formed due to hyperpycnal flows (Lamb et al., 2010). To explain the presence of boulders on ridge tops (Figure 7B), we point to recent studies that show subaqueous debris flows can transport boulders over substantial distances (~10 km) in submarine canyons (Talling et al., 2010). Such events may be generated by seismic activity (Ribó et al., 2024) which could be impact events on Mars.

5.2 Case study 2: Harris crater, Mars

The plains northeast of Hellas Planitia have drawn a lot of research interest due to the diversity of interior deposits within crater basins. Martian alluvial fans are geographically restricted, with one regional cluster of megafans (10–40 km radial length)

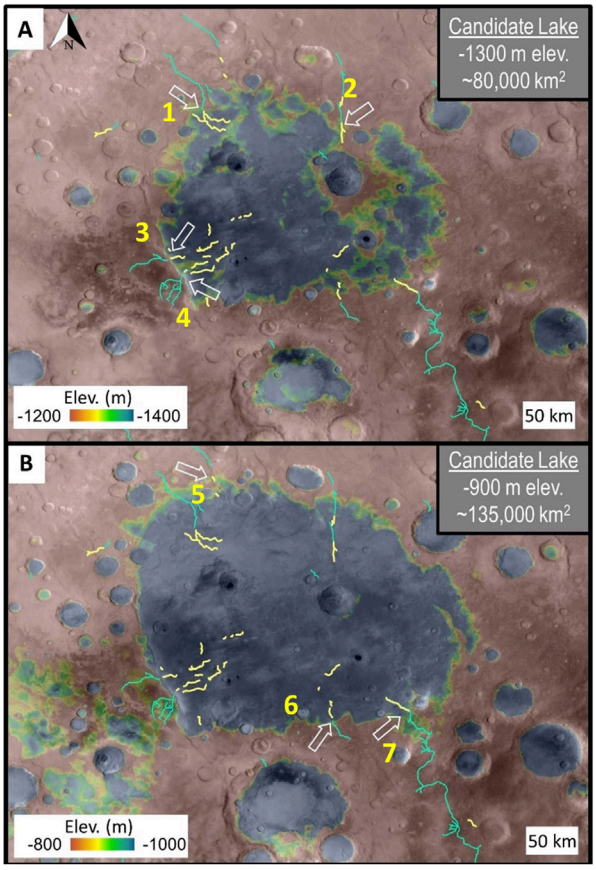

FIGURE 8
Candidate lake levels at Phison Patera, Mars. Color ramp used for MOLA elevation is stretched to a 200 m interval centered around possible water level (yellow band is ~30 m elevation range) at **(A)** −1,300 m elevation and **(B)** −900 m elevation. Lines in all panels are from Hynek (2016) mapping of valley networks (light blue lines) and Davis et al. (2019) mapping of ridges interpreted as paleochannel ridges (yellow lines). White arrows mark locations where the transition from valley network to paleochannel ridge coincides with the possible lake level illustrated. Yellow numbers correspond to ID# in Supplementary Table S1.

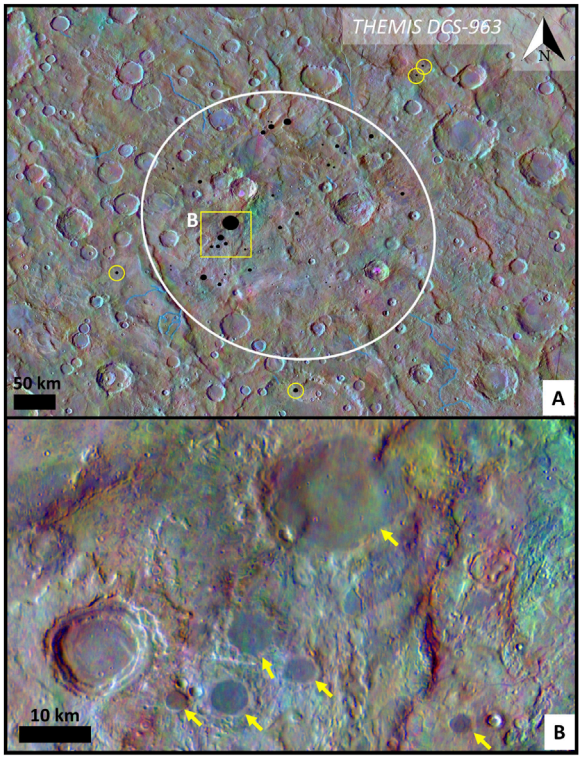

FIGURE 9
(A) White oval outlines the regional concentration of indurated rimless crater fill features (black dots). Within the area shown only four indurated crater fill features are mapped outside of the proposed paleolake site (yellow circles). Basemap is THEMIS DCS-963 mosaic overlain on THEMIS daytime infrared global mosaic (Edwards et al., 2011 ab) with mapped valley networks (blue lines) from Hynek et al. (2010). Center of figure is near 30.0°N, 47.5°E **(B)** Subscene of THEMIS DCS-963 to illustrate the purplish color of rimless round features interpreted as indurated crater fill. Figures created through JMARS: NASA/JPL-Caltech/Arizona State University.

present within craters in Southwesten Tyrrhena Terra, including Harris crater (Moore and Howard, 2005; Wilson et al., 2021). Very few (N = 2) of the intracrater fans in this region are interpreted to be deltaic (e.g., Wilson et al., 2021). Nevertheless, multiple closed basin lakes are identified in this region, all of which lack a triangular fan deposit (Goudge et al., 2015). Some craters have layered sedimentary deposits (Malin and Edgett, 2000) containing hydrated minerals that are thought to be lacustrine in origin (Ansan and Mangold, 2004; Wilson et al., 2007).

Harris crater has a diameter of 82 km and is located at ~ 21.9°S, 66.8°E (Figure 10). The Harris impact event occurred between Early Hesperian and Early Amazonian (~3.7 to ~3.3 Ga) and is part of a fresher class of craters thought to postdate the main era of valley network activity (Mangold et al., 2012). Gullikson et al. (2023) mapped water-related landforms in the northern region of Hellas Planitia, including at Harris crater (Figure 10). Five intracrater fans at Harris crater were previously interpreted as alluvial fans (Figure 11; Williams et al., 2011; Anderson et al., 2023; Wilson et al., 2021). In this study, we evaluate if there was lacustrine overprinting of the original alluvial deposits.

5.2.1 Assessment of candidate lake levels at Harris crater

We evaluated two candidate lake levels based on onset elevation of paleochannel ridges and assessed the consistency with elevations at which valley networks terminate (Supplementary Figure S7). Paleochannel ridges were mapped on the southern and northeastern fans by Gullikson et al. (2023); yellow lines on Figure 10). These ridges have relief of <10 m (Supplementary Figure S8). On the southern alluvial fan, isolated paleochannel ridges originate mid-fan and are not associated with negative-relief valleys (Figure 11B). These linear paleochannel ridges are few in number and parallel to each other. On the northeastern alluvial fan complex, paleochannel ridges initiating at the fan apex and in some cases are continuous from valley networks in the wall catchment. Paleochannel ridges radiate downslope in bifurcating segments ~200 m long, for a total distance of ~15 km. Williams et al. (2011) identified three

TABLE 1 Summary of observations and evaluation of martian candidate lake levels.

Site	Lake level (m)	Landform match (<30 m)[1]	Landform nearby (<90 m)	Region	Region	Region	Evaluation
Phison Patera	−900	2 VN—PR	—	Paleolake deposits	Ponding spillover	—	Plausible
	−1,300	4 VN—PR	—				Likely
Harris Crater	−1900	3 VN	3 VN	—	Evaporite minerals	Desiccation polygons	Unlikely
	−2,200	4 PR	4 VN	Alluvial fan scarp			Plausible

[1]VN = valley network, PR = paleochannel ridge.

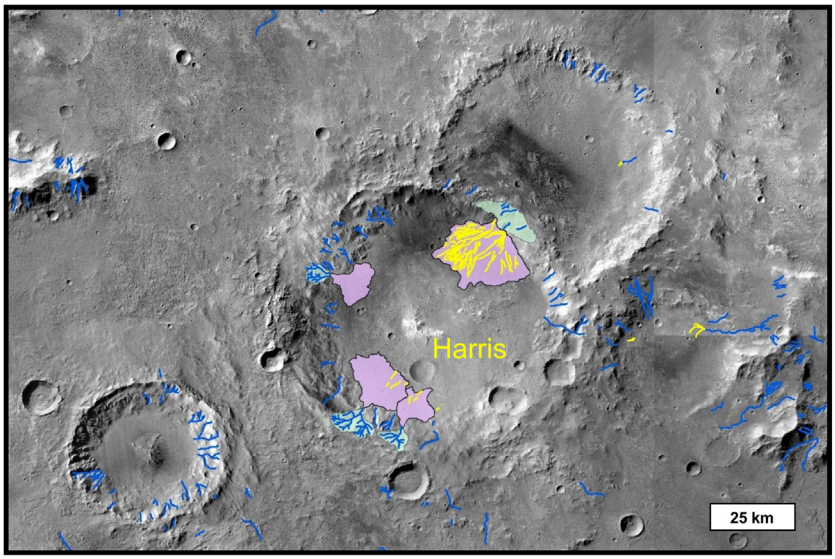

FIGURE 10
Context map for Harris crater, an ~80 km diameter crater located northeast of Hellas Planitia, at ~ 21.9°S, 66.8°E. Gullikson et al. (2023) mapped fans (purple) and catchments (green), valley networks (blue lines) and paleochannel ridges (yellow lines).

depositional units that included fluvial processes and a late-stage, boulder-rich debris (Figure 11A).

First, we used the maximum paleochannel ridge elevation on the southwestern fans (−2,200 m; lower white arrow in Figure 12A), covering an area of ~2,140 km^2. This elevation is consistent for two paleochannel ridges (Figure 11B), and it matches (<30 m) a few paleochannel ridges that originate on the mid-fan of the northeastern alluvial fan (green arrow in Figure 12A). Also this elevation is near (<90 m) four valley network terminations on the western crater wall (pink arrows in Figure 12A; Supplementary Figure S9). One alluvial fan deposit with a terminal scarp (orange arrow in Figure 12A) could be additional evidence of a shoreline, however, multiple escarpments on the crater floor cross contours and have an ambiguous origin.

Second, using the elevation of the northeastern alluvial fan apices (−1900 m; white arrow Figure 12B) establishes the maximum lake area and depth (2,680 km^2, 1,400 m). This elevation was selected as an upper bound test. This potential water level corresponds to the termination of several valley networks on the northeastern and southern side of Harris crater, matching three and near three inlets (blue and pink arrows, respectively, in Figure 12B).

5.2.2 Interpretation: Harris crater, Mars

We propose that the Harris crater ridges may be preservation of paleochannels with two disparate origins, but both associated with a low-energy. depositional setting. The northeast fan is composed of heavily deflated alluvial fan deposits where wind erosion has removed finer-grained sediment producing networks of superposed distributary channels preserved in inverted relief (e.g., raised channels; Figure 11A). In contrast, we suggest the southern alluvial fan distal ridges are sublacustrine (Figure 11B), forming in positive relief mid-fan associated with a paleolake, similar to the origin of subaqeuous ridges at Lake Coyote, CA. Consistent with deposition at the river-to-lake transition, there are boulder deposits locally present on the paleochannel ridges (Figure 11C), although limited meter-scale images of the southern alluvial fan restrict detection of coarse sediment. Potentially, the northeast mid-fan ridges (green arrow in Figure 12A) also formed by this mechanism and overprinted a partially submerged northeastern

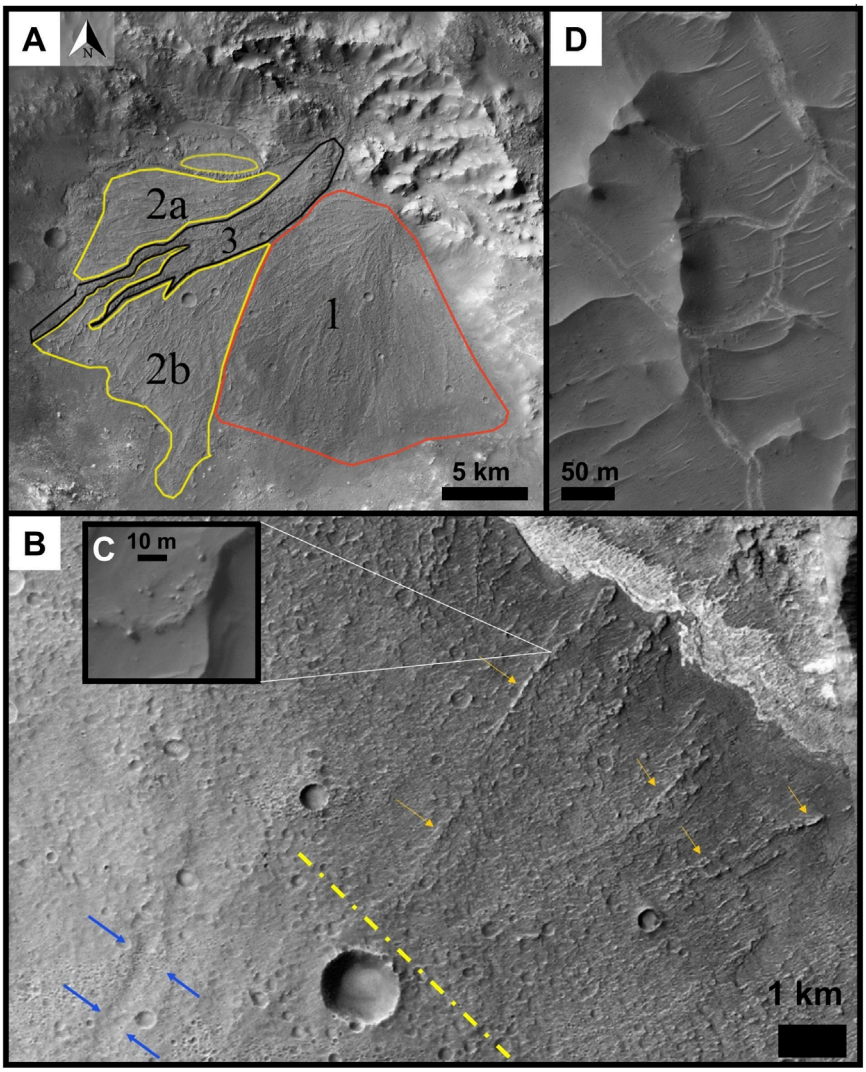

FIGURE 11
Examples of alluvial fan surfaces in Harris crater from CTX global mosaic (Dickson et al., 2024). **(A)** Harris crater's northeastern fan has multiple lobes, as mapped by Williams et al. (2011). Numbers denote the depositional sequence. There is a tonal difference between the dark lobe 1 and the lighter lobe 2, in addition to cross-cutting relationships to distinguish the lobes. The third deposit is boulder-rich and interpreted as a late-stage debris flow. **(B)** The distal reaches of the southwestern fan has linear ridges (orange arrows) downslope from the −2,200 m contour (dashed yellow line) and not associated with broad valleys (blue arrows). These ridges are interpreted as subaqueously formed paleochannels. White deposits at upper right could be evaporite salts, which are commonly bright in CTX images. **(C)** Boulders are present in places on ridge. **(D)** Light-toned polygonal pattern on crater floor is consistent with desiccation cracks. **(A, B)** are subscenes of CTX global mosaic, and **(C, D)** are subscenes of HiRISE ESP_018527_1575.

alluvial fan, but this interpretation cannot be distinguished from eroded telescoping alluvial fan deposits in the available data. Supplementary evidence of a paleolake at Harris crater includes: 1) light-toned deposits on a crater floor (Figure 11B) that has a chloride spectral signature (Bickel et al., 2024), consistent with evaporite deposits (Osterloo et al., 2008; 2010; Hynek et al., 2015); and 2) topographic benches that could be lake terraces, although further work is needed to refine this interpretation.

Differences in the alluvial fans on the north and south side of Harris crater reflect their respective source regions. Because the northeastern rim of Harris crater coincides with a pre-existing crater rim (Figure 10), the Harris impact event may have reworked those upturned rocks resulting in a catchment comprised of highly erodible material. Poorly integrated drainage within the catchment suggests relatively coarse grain size in fan deposits, and supports the interpretation of clast armored raised channels in the northeastern alluvial fan complex. In contrast, the catchment for the southern fan is bedrock of the Harris crater rim. Valley networks are integrated in the southern catchment (Figure 10), suggesting comminution and a range of sediment sizes available for transport. A fining downfan sequence may have supported the retention of impact craters in fan deposits (Figure 11B). Late-stage flows across this fan surface could have encountered rising water in a lake, generating distal linear ridges on the margins of the southern fan (Figure 11B).

We speculate that groundwater may have been a source of water helping to stabilize lake level at Harris crater. Figure 11D

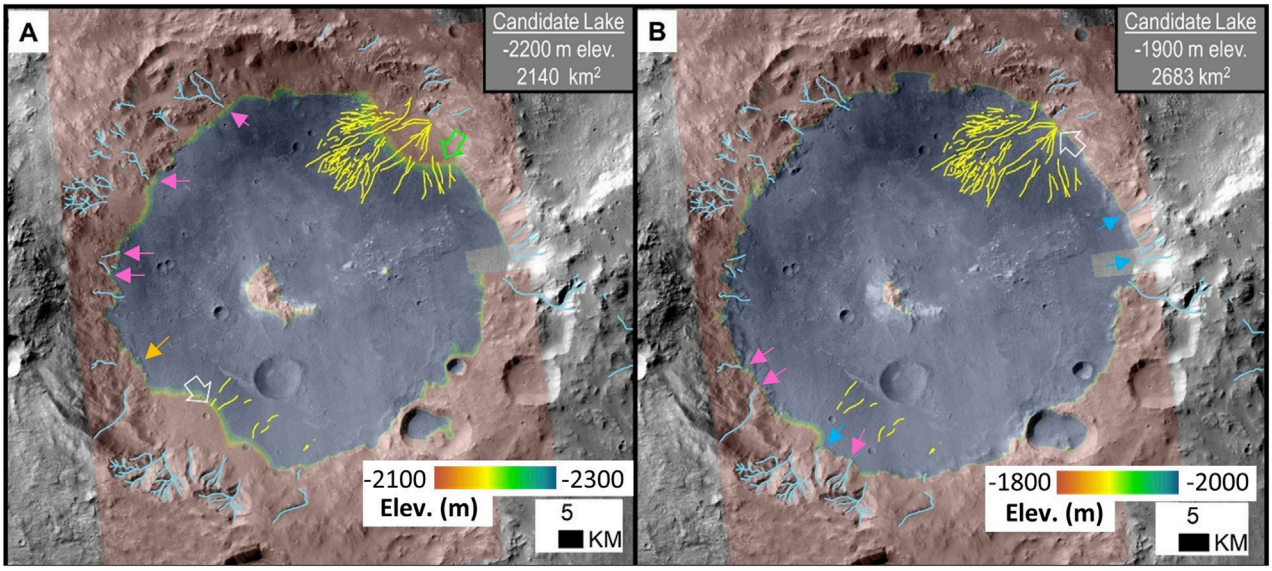

FIGURE 12
Candidate lake levels at Harris crater, Mars. Color ramp used for CTX DEM elevation is stretched to a 200 m interval centered around possible water level (yellow band is ~30 m elevation range). Shoreline elevation is defined at white open arrows for two cases (–2,200 m in **(A)**, and –1900 m in **(B)**. Solid arrows mark features that are close in elevation to the candidate lake level: valley network inlets at consistent (<30 m) elevations have blue arrows and nearby elevations (<90 m) have pink arrows, and in **(A)**, green arrows marks paleochannel ridges that originate mid-fan at an elevation close to the evaluated –2,200 m shoreline, and orange arrow marks fan with terminal scarp. Lines in all panels are from Gullikson et al. (2023) mapping of valley networks (light blue lines) and ridges interpreted as raised channels (yellow lines).

illustrates 50–100 m wide polygonal crack patterns on the crater floor reminiscent of shrinkage polygons formed through desiccation (El Maarry et al., 2010). Their perimeter is characterized by paired ridges bounding a crack, a configuration similar to groundwater upwelling exploiting desiccation polygons at the Great Salt Lake, Utah (Vanden Berg, 2019). Global-scale hydrological models show groundwater upwelling at this location is only associated with a wet hydrological regime (Andrews-Hanna and Lewis, 2011), suggesting that if groundwater were present at Harris crater it either resulted from local conditions, or global-scale processes occasionally persisted well past the Noachian era.

In the synthesis of observations, we find the higher candidate lake level (−1900 m) an unlikely marker of a paleolake at Harris crater because there is insufficient ancillary morphology to suggest water levels ever reached this maximum height and it is difficult to fit within a landform development sequence (Table 1). The valley network terminations associated with this elevation lack terminal triangular deposits; rather these inlets may have been buried with intracrater fill, possibly lacustrine deposits associated with a lower lake level. In sum, there is weak evidence to support a −1900 m lake level.

Based on our analysis, a paleolake at Harris crater is plausible (−2,200 m level) but is a non-unique model that fits available data. An evolutionary scenario at Harris crater could be subdivided into three periods by depositional environment. Phase 1 involved alluvial fan aggradation emplacing the bulk of sediment by volume within the basin, including lobes 1 and 2 of the northeast fan complex (Figure 11A). Phase 2 was a transgressive lake period. Lake level may have reached −2,200 m (Figure 12A), based on consistency of paleoshoreline indicators, phase 3 returned to alluvial processes, including the debris flow deposits in lobe 3 of the northeast fan complex, but it involved far less material mobilized than in phase 1. This depositional sequence—early alluvial sedimentation, intermediate lacustrine deposition, late-stage alluvial activity—is consistent with superposition relationships at Harris crater.

6 Discussion

6.1 Terrestrial subaqueous ridges

6.1.1 Lake Coyote paleochannel ridges

The Minneola fluvial plain gravel-capped paleochannel ridges have a composite origin (Hagar, 1966; Dudsah, 2006; Miller, 2018). Although Lake Coyote paleochannel ridges extend >15 km from the Mojave River, it is only the distal ~3 km spanning ~5 m elevation that are interpreted as subaqueously formed paleochannel ridges. Most of the paleochannel ridges on the Minneola floodplain (~80% by length) are raised channels, formed *via* differential erosion of Mojave River deposits. Critically, this example illustrates that paleochannel ridges can be a lake margin landform.

The case for subaqueous paleochannel ridge formation at the river to lake confluence is substantiated at Lake Coyote by multiple pieces of evidence that are difficult to identify or not detectible in existing data for Mars. The interpretation was founded on the sedimentology: interfingered fluvial gravels and lacustrine silt deposits with shallow water fossils (*Anodonta* shells). The paleochannel ridge planform at the lake margin is varied, from the eastern bulbous terminations to the western complex of radial ridges merging with an arcuate barrier beach (Figure 3B).

Superposition or stacking patterns of the ridges may not be resolved in topographic data and were only identified through facies contacts in excavated trenches combined with radiocarbon dates. Furthermore, the Lake Coyote paleochannel ridges merge with lakeshore landforms, an example of compound landforms where fluvio-lacustrine depositional settings meet. Absent ground truth, similar planimetric patterns in remotely sensed data may suggest alternative interpretations, such as raised channels or distributary paleochannels.

6.1.2 Terrestrial paleochannel ridges and paleolakes

Most raised channels ('inverted channels') recognized on Earth formed in depositional settings where channel deposits could become more resistant than surrounding materials (e.g., enhanced cementation, deposition of coarse clasts). Some studies have noted raised channels located near past lakes. Sites include paleolake Tushka in Egypt (Maxwell et al., 2010), Lake Bonneville in Utah (Oviatt et al., 2003), Lake Manix in California (Miller et al., 2018), the Qaidam Basin in China (e.g., Li et al., 2025), and the salars in the Chilean Atacama Desert (Morgan et al., 2014). However, very few published studies have specifically linked raised channel locations directly to lacustrine shorelines, and these are associated with clast-armored raised channels. It is unknown whether other types of inverted channels may also be linked to paleoshorelines.

In addition to the subaqueous paleochannel ridges at Lake Coyote (Miller et al., 2018), we are aware of only one other example of raised channels associated with a specific lake level. Williams et al. (2021) proposed that gravel-capped ridges at Salar de Llamara in the Chilean Atacama Desert may correspond to a paleoshoreline. These Atacama clast-armored ridges are virtually indistinguishable from the Lake Coyote raised channels in surface observations. Both are examples of unconsolidated, clast-armored raised channels.

Unfortunately, this type of raised channel (clast-armored) is not readily identifiable in remotely sensed data. In fact, two types of paleochannel ridges are present at Salar de Llamara, but they appear nearly identical in satellite images. Most of the paleochannel ridges are gravel-capped, but some are sulfate-cemented (Morgan et al., 2014; Williams et al., 2021). Where junctions are preserved, the gravel-capped paleochannel ridges exhibit a distributary (downslope branching) planimetric pattern, whereas the sulfate-capped paleochannel ridges have a contributory pattern (downslope merging). Differentiating the two varieties could also be possible using high resolution (decimeter-scale) topographic data based on cross-sectional shape: gravel-armored inverted channels exhibit a rounded shape, in contrast to the rectangular form of cemented paleochannel ridges (e.g., Williams et al., 2021).

Clast-armored raised channels (i.e., with differential resistance provided only by grain size rather than cementation) are rarely documented in the terrestrial literature. In the global inventory of Zaki et al. (2021), clast-armored raised channels constitute <5% of cases, and are found in hyperarid settings. Although there are few examples of this variety, there are cases of clast-armored ridges that formed well removed from lacustrine settings, such as in low stream order river tributaries (e.g., Marchetti et al., 2012). Thus, this landform type is not diagnostic of a lacustrine depositional setting.

6.2 Subaqueous ridges on Mars

Drawing upon a terrestrial analog, we demonstrate that some depositional ridges on Mars may have formed subaqueously in lakes. This new insight paves the way for future studies to use this landform in detailed lake hydrograph reconstructions. On Mars, consistency tests were passed in evaluating two case studies, substantiating the plausibility of subaqueously-formed ridges. We examined commonalities between paleochannel ridge onset elevation and termination points of valley networks to assess possible paleolake levels within topographic basins. Additional morphological evidence of paleolake deposits was present at both sites: indurated crater fill at Phison Patera, evaporite salts and desiccation polygons at Harris crater. Our two examined sites differ in physical scale and energy setting, raising the prospect for considering constructional paleochannel ridges in detailed geologic studies.

We find the case for a paleolake at Phison Patera stronger than the one at Harris crater and acknowledge that the available data does not support a unique interpretation (Table 1). Critically, both sites retain a valid alternative explanation, namely the original raised channel hypothesis. A subaqueous ridge origin for some ridges at the studied locations is a reasonable interpretation with a comparable level of confidence as previous findings with the available observational evidence. Future work could further evaluate paleolake feasibility through three-dimensional modeling of fluvial and groundwater inputs. Mineralogical signatures of salts in spectral data, especially if localized to the basin, would further corroborate a paleolake interpretation.

This proof-of-concept study provides a basis for examining the formation setting of other martian paleochannel ridges, especially in cases where they converge within a topographic basin as would be consistent with a subaqueous origin. Geomorphic mapping is a way to synthesize the geologic context. Factors to consider include the relationship of paleochannel ridges to modern topography, the regional drainage pattern, the spatial distribution of water-formed minerals, and the presence of lacustrine landforms (e.g., deltas, barrier beaches, lake terraces, layered sedimentary deposits, shrinkage polygons, *etc.*).

Recognition of paleochannel ridges as lake level indicators would critically inform 1) identification of additional paleolake sites, especially in degraded terrains, and 2) future hydrograph reconstruction through constraints on lake extent and water level sequence. The significance of this finding is that it introduces a new shoreline-associated landform for reconstructing lake-level fluctuations, a tool for deepening our understanding of hydrology and habitability on Mars. By assessing paleochannel ridges as shoreline indicators, new insights into the regional and/or global martian climate oscillations can be probed.

Data availability statement

The datasets presented in this study can be found in online repositories. The names of the repository/repositories and accession number(s) can be found in the article/Supplementary Material.

Author contributions

RW: Conceptualization, Data curation, Formal Analysis, Funding acquisition, Investigation, Methodology, Project administration, Resources, Validation, Visualization, Writing – original draft, Writing – review and editing. RI: Data curation, Investigation, Validation, Writing – review and editing. DB: Validation, Data curation, Writing – review and editing. JH: Data curation, Writing – review and editing.

Funding

The author(s) declare that financial support was received for the research and/or publication of this article. This research was supported by NASA's Mars Data Analysis Program grants to RW, principally #80NSSC20K0944 supplemented by #0NSSC19K1216, NASA's Solar System Workings program #NNX13AG83G for the terrestrial analog, and funds to support the Mars Odyssey-THEMIS Extended Mission program (NASW-00002) for mapping indurated crater fill.

Acknowledgments

We acknowledge editor Alberto Farién for handling our manuscript. This work was substantially improved by the constructive criticism from two reviewers and we appreciate their time and feedback. The authors are extremely grateful to David Miller (USGS) for detailed discussion of the Lake Coyote site based on his team's extensive fieldwork throughout the Lake Manix basin. Data produced in this project are archived at https://doi.org/10.5066/P9I1QO1U. This project utilized JMARS for data analysis and figure generation (https://jmars.asu.edu; Christensen et al., 2009).

Conflict of interest

The authors declare that the research was conducted in the absence of any commercial or financial relationships that could be construed as a potential conflict of interest.

Generative AI statement

The author(s) declare that no Generative AI was used in the creation of this manuscript.

Any alternative text (alt text) provided alongside figures in this article has been generated by Frontiers with the support of artificial intelligence and reasonable efforts have been made to ensure accuracy, including review by the authors wherever possible. If you identify any issues, please contact us.

Publisher's note

Supplementary material

The Supplementary Material for this article can be found online at: https://www.frontiersin.org/articles/10.3389/fspas.2025.1666811/full#supplementary-material

References

Allen, J. R. L. (1965). A review of the origin and characteristics of recent alluvial sediments. *Sedimentology* 5 (2), 89–191. doi:10.1111/j.1365-3091.1965.tb01561.x

Anderson, R. B., Williams, R. M. E., Gulikson, A. G., and Nelson, W. (2023). Inverted relief and morphology of intracrater alluvial fans north of Hellas Basin. *Icarus* 394 (115122), 22. doi:10.1016/j.icarus.2022.115122

Andrews-Hanna, J., and Lewis, K. W. (2011). Early Mars hydrology: 2. Hydrological evolution in the Noachian and Hesperian epochs: *J. Geophys. Res.*, 116 E02007. doi:10.1029/2010JE003709

Ansan, V., and Mangold, N. (2004). "Impact crater paleolakes in Hellas and, Thaumasia areas, M," in *Paper presented at Second Conference on Early, and Mars*. Houston, Texas: Lunar and Planetary Institute. Abstract #8006.

Antoniadi, E. M. (1930). *La Planéte Mars*. Paris: Hermann and Co.

Ashmore, P. (2013). "Morphology and dynamics of braided rivers," in *Treatise on Geomorphology, volume 9: Fluvial Geomorphology*. Editor E. E. Wohl (London: Academic Press), 289–312. doi:10.1016/B978-0-12-374739-6.00242-6

Aslan, A., and Blum, M. D. (1999). Constrasting styles of Holocene avulsion, Texas Gulf Coastal Plain, USA. *Spec. Publs Int. Ass. Sediment.* 28, 193–209. doi:10.1002/9781444304213.ch15

Baran, Z. J., and Cardenas, B. T. (2025). Modeling Lake Bonneville paleoshoreline erosion at Mars-like rates and durations: Implications for the preservation of erosional martian shorelines and viability as evidence for a martian ocean. *J. Geophys. Res. Planets* 130 (4), e2024JE008851. doi:10.1029/2024JE008851

Benson, L. V., and Paillet, F. L. (1989). The use of total lake-surface area as an indicator of climatic change: examples from the Lahontan Basin. *Quat. Res.* 32, 262–275. doi:10.1016/0033-5894(89)90093-8

Beyer, R. A., Alexandrov, O., and McMichael, S. (2018). The Ames Stereo Pipeline: NASA's open source software for deriving and processing terrain data. *Earth Space Sci.* 5 (9), 537–548. doi:10.1029/2018EA000409

Bickel, V. T., Thomas, N., Pommerol, A., Tornabene, L. L., El-Maarry, M. R., and Rangarajan, V. G. (2024). A global dataset of potential chloride deposits on Mars as identified by TGO CaSSIS. *Sci. Data* 11 (845), 845. doi:10.1038/s41597-024-03685-3

Blum, M. D., and Price, D. M. (1988). "Quaternary alluvial plain construction in response to glacio-eustatic and climatic controls, Texas Gulf Coastal Plain,"*Relative role of Eustasy, Climate, and Tectonism in Continental Rocks*. Editors K. W. Shanley, and P. J. McCabe (Tulsa, OK: Special Publication of SEPM), 59, 31–48. doi:10.2110/pec.98.59.0031

Bradley, R. S. (2015). *Paleoclimatology: reconstructing climates of the Quaternary*. New York: Academic Press, 696. doi:10.1016/C2009-0-18310-1

Bridge, J. S. (1984). Large-scale facies sequences in alluvial overbank environments. *J. Sediment. Res.* 54 (2), 583–588. doi:10.1306/212F8477-2B24-11D7-86480001 02C1865D

Bridge, J. S. (2003). *Rivers and floodplains: forms, processes, and sedimentary record*. Oxford, UK: Blackwell Publishing, 600.

Bridge, J. S., and Leeder, M. R. (1979). A simulation model of alluvial stratigraphy. *Sedimentology* 26 (5), 617–644. doi:10.1111/j.1365-3091.1979.tb00935.x

Bunte, K., and Abt, S. R. (2001). *Sampling surface and subsurface particle-size distributions in wadable gravel- and cobble-bed streams for analyses in sediment transport, hydraulics, and streambed monitoring. Gen. Tech. Rep. RMRS-GTR-74*. Fort Collins, CO: U.S. Department of Agriculture, Forest Service, Rocky Mountain Research Station, 428. doi:10.2737/RMRS-GTR-74

Cabrol, N., and Grin, E. A. (1999). Distribution, classification and ages of martian impact crater lakes. *Icarus* 142, 160–172. doi:10.1006/icar.1999.6191

Caravaca, G., Dromart, G., Mangold, N., Gupta, S., Kah, L. C., Tate, C., et al. (2024). Depositional facies and sequence stratigraphy of Kodiak Butte, Western Delta of Jezero Crater, Mars. *J. Geophys. Res. Planets* 129 (4), e2023JE008205. doi:10.1029/2023JE008205

Cardenas, B. T., Mohrig, D., and Goudge, T. A. (2018). Fluvial stratigraphy of valley fills at Aeolis Dorsa, Mars: evidence for base-level fluctuations controlled by a downstream water body. *GSA Bull.* 130 (3-4), 484–498. doi:10.1130/B31567.1

Cardenas, B. M., Mohig, D., Goudge, T., Hughes, C., Levy, J., Swanson, T., et al. (2020). The anatomy of exhumed river-channel belts: bedform to belt-scale river kinematics of the Ruby Ranch Member, Cretaceous Cedar Mountain Formation, Utah, USA. *Sedimentology* 67 (7), 3655–3682. doi:10.1111/sed.12765

Carr, M. H. (1995). The martian drainage system and the origin of valley networks and fretted channels. *J. Geophys. Res. Planets* 100 (E4), 7479–7507. doi:10.1029/95JE00260

Carr, M. H. (1996). *Water on Mars*. New York: Oxford University Press, 248.

Carr, M. H., and Head, J. W. I. (2010). Geologic history of Mars. *Earth Planet. Sci. Lett.* 294, 185–203. doi:10.1016/j.epsl.2009.06.042

Christensen, P. R., Bandfield, J. L., Hamilton, V. E., Ruff, S. W., Kieffer, H. H., Titus, T., et al. (2001). Mars Global Surveyor Thermal Emission Spectrometer experiment: investigation description and surface science results. *J. Geophys. Res.* 106 (23), 23823–23871. doi:10.1029/2000JE001370

Christensen, P. R., Engle, E., Anwar, S., Dickenshied, S., Noss, D., Gorelick, N., et al. (2009). JMARS – a planetary GIS, AGU fall meeting abstracts. Available online at: http://adsabs.harvard.edu/abs/2009AGUFMIN22A.06C (Accessed June 1, 2025).

Church, M. (2006). Bed material transport and the morphology of alluvial river channels. *Annu. Rev. Earth Planet. Sci.* 34, 325–354. doi:10.1146/annurev.earth.33.092203.122721

Clarke, J. D. A., Pain, C. F., and Rupert, S. (2020). Complex expressions of inverted and exhumed relief in central Utah, and some martian counterparts. *Phys. Geogr.* 18. doi:10.1080/02723646.2020.183916

Cuevas Martínez, J. L. C., Prerez, L. C., Marcuello, A., Cazo, P. A., Carpio, M. M., and Bellmunt, F. (2010). Exhumed channel sandstone networks within fluvial fan deposits from the Oligo-Miocene Caspe Formation, South-East Ebro Basin (North-East Spain). *Sedimentology* 57, 162–189. doi:10.1111/j.1365-3091.2009.01096.x

Davis, J. M., Balme, M. R., Grindrod, P. M., Williams, R. M. E., and Gupta, S. (2016). Extensive Noachian fluvial systems in Arabia Terra: Implications for early martian climate. *Geology* 44 (10), 847–850. doi:10.1130/G38247.1

Davis, J. M., Grindrod, P. M., Fawdon, P., Williams, R. M. E., Gupta, S., and Balme, M. (2018). Episodic and declining fluvial processes in Southwest Melas Chasma, Valles Marineris, Mars. *J. Geophys. Res. Planets* 123, 2527–2549. doi:10.1029/2018JE005710

Davis, J. M., Gupta, S., Balme, M. R., Grindrod, P. M., Fawdon, P., Gupta, S., et al. (2019). A diverse array of fluvial depositional systems in Arabia Terra: evidence for mid-Noachian to early Hesperian rivers on Mars. *J. Geophys. Res. Planets* 124, 1913–1934. doi:10.1029/2019JE005976

Davis, J. M., Sanjeev, G., Grindrod, P. M., Banham, S. G., Wilson, S. A., Rudolph, A., et al. (2025). Late-stage aqueous activity at Gale Crater, Mars, recorded by sediment fans eroded from Aeolis Mons. *J. Geophys. Res. Planets.* 130 (3). doi:10.1029/2024JE008808

Day, M., Anderson, W., Kocurek, G., and Mohrig, D. (2016). Carving intracrater layered deposits with wind on Mars. *Geophys. Res. Lett.* 43 (6), 2473–2479. doi:10.1002/2016GL068011

Dickeson, Z. I., Grindrod, P. M., Davis, J. M., Crawford, I., and Balme, M. R. (2022). Hydrological history of a palaeolake and valley system on the planetary dichotomy in Arabia Terra, Mars. *J. Geophys. Res. Planets* 127, e2021JE007152. doi:10.1029/2021JE007152

Dickson, J. L., Lamb, M. P., Williams, R. M. E., Hayden, A. T., and Fischer, W. W. (2021). The global distribution of depositional rivers on early Mars. *Geology* 49 (5), 504–509. doi:10.1130/G48457.1

Dickson, J. L., Ehlmann, B. L., Kerber, L., and Fassett, C. I. (2024). The global Context Camera (CTX) mosaic of Mars: a product of information-preserving image data processing. *Earth Space Sci.* 11, e2024EA003555. doi:10.1029/2024EA003555

Dudsah, S. L. (2006). Preliminary surficial geologic map of a Calico Mountains piedmont and part of Coyote Lake, Mojave Desert, San Bernardino County, California. Flagstaff, AZ: US Geological Survey Open-File Report 2006-1090, 44. doi:10.3133/ofr20061090

Edgett, K. S. (2005). The sedimentary rocks of Sinus Meridiani: Five key observations from data acquired by the Mars Global Surveyor and Mars Odyssey orbiters. *Int. J. Mars Sci. Explor.* 1, 5–58. doi:10.1555/mars.2005.0002

Edgett, K. S., Bennett, K. A., Edgar, L. A., Edwards, C. S., Fairén, A. G., Fairén, A. G., et al. (2020). Extraformational sediment recycling on Mars. *Geosphere* 16 (6), 1508–1537. doi:10.1130/GES02244.1

El Maarry, M. R., Markiewicz, W. J., Mellon, M. T., Goetz, W., Dohm, J. M., and Pack, A. (2010). Crater floor polygons: desiccation patterns of ancient lakes on Mars? *J. Geophys. Res. Planets* 115, E10006. doi:10.1029/2010JE003609

Fan, Q., Ma, H., and Hou, G. (2011). Late Pleistocene lake and glaciation evolution on the northeastern Qinghai–Tibetan Plateau: a review. *Environ. Earth Sci.* 66 (2), 625–634. doi:10.1007/s12665-011-1271-x

Fassett, C. I., and Head, J. W., III (2008). Valley network-fed, open-basin lakes on Mars, distribution and implications for Noachian surface and subsurface hydrology. *Icarus* 198, 37–56. doi:10.1016/j.icarus.2008.06.016

Fassett, C. I., and Head III, J. W. (2007). Layered mantling deposits in northeast Arabia Terra, Mars: Noachian-Hesperian sedimentation, erosion, and terrain inversion. *J. Geophys. Res. Planets* 112 (E8). doi:10.1029/2006JE002875

Fawdon, P., Gupta, S., Davis, J. M., Warner, N. H., Adler, J. B., Balme, M. R., et al. (2018). Hypanis Valles delta: the last high stand of an ocean on early Mars? *Earth Planet. Sci. Lett.* 500, 225–241. doi:10.1016/j.epsl.2018.07.040

Fergason, R. L., Hare, T. M., and Laura, J. (2018). HRSC and MOLA blended digital elevation model at 200m v2. Astrogeology PDS Annex, U.S. Geological Survey. Available online at: https://astrogeology.usgs.gov/search/map/mars_mgs_mola_mex_hrsc_blended_dem_global_200m. https://planetarymaps.usgs.gov/mosaic/Mars/HRSC_MOLA_Blend/Mars_HRSC_MOLA_BlendDEM_Global_200mp_v2.tif.

Fielding, C. R. (2007). "Sedimentology and stratigraphy of large river deposits: recognition in the ancient record, and distinction from "incised valley fills"," in *Large Rivers: Geomorphology and Management*. Editor A. Gupta (Chichester, UK: John Wiley and Sons, Ltd.), 97–113. doi:10.1002/9780470723722.ch7

Fisk, H. N. (1944). *Geological investigation of the alluvial valley of the lower Mississippi River, United States Army Corps of Engineers, Mississippi River Commission, 78p. scale 1:500,000*. Vicksburg: U.S. Army Corps of Engineers.

Fisk, H. N. (1952). Mississippi River valley geology relation to river regime. *Trans. Am. Soc. Civ. Eng.* 117 (1), 667–682. doi:10.1061/TACEAT.0006733

Foix, N., Allard, J. O., Paredes, J. M., and Giacosa, R. E. (2012). Fluvial styles, palaeohydrology and modern analogues of an exhumed, Cretaceous fluvial system: Cerro Barcino Formation, Cañadón Asfalto Basin, Argentina. *Cretac. Res.* 34, 298–307. doi:10.1016/j.cretres.2011.11.010

Frey, H. V., Roark, J. H., Shockey, K. M., Frey, E. L., and Sakimoto, S. E. H. (2002). Ancient lowlands on Mars. *Geophys. Res. Lett.* 29 (10). doi:10.1029/2001GL013832

Gearon, J. H., and Edmonds, D. A. (2025). River avulsion precursors encoded in alluvial ridge geometry. *Geophys. Res. Lett.* 52 (8), e2024GL114047. doi:10.1029/2024GL114047

Gilbert, K. G. (1890). *Lake Bonneville. Monograph 1*. Washington, DC: United States Geological Survey, 438. doi:10.3133/m1

Godsey, H. S., Currey, D. R., and Chan, M. A. (2005). New evidence for an extended occupation of the Provo Shoreline and implications for regional climate change, Pleistocene Lake Bonneville, Utah, USA. *Quat. Res.* 63, 212–223. doi:10.1016/j.yqres.2005.01.002

Google Earth Pro (2024). *Version 7.3.6.9796*. Available online at: https://earth.google.com/web/.

Goudge, T. A., Mustard, J. F., Head, J. W., and Fassett, C. I. (2012). Constraints on the history of open-basin lakes on Mars from the composition and timing of volcanic resurfacing. *J. Geophys. Res. Planets* 117 (E12). doi:10.1029/2012JE004115

Goudge, T. A., Aureli, K. L., Head, J. W., Fassett, C. I., and Mustard, J. F. (2015). Classification and analysis of candidate impact crater-hosted closed-basin lakes on Mars. *Icarus* 260, 346–367. doi:10.1016/j.icarus.2015.07.026

Goudge, T. A., Milliken, R. E., Head, J. W., Mustard, J., and Fassett, C. I. (2017). Sedimentological evidence for a deltaic origin of the western fan deposit in Jezero Crater, Mars and implications for future exploration. *Earth Planet. Sci. Lett.* 458, 357–365. doi:10.1016/j.epsl.2016.10.056

Grant, J. A., and Wilson, S. A. (2011). Late alluvial fan formation in southern Margaritifer Terra, Mars. *Geophys. Res. Lett.* 38 (L08201). doi:10.1029/2011GL046844

Grant, J. A., Golombek, M. P., Grotzingerc, J. P., Wilson, S. A., Watkins, M. M., Vasavada, A. R., et al. (2010). The science process for selecting the landing site for the 2011 Mars Science Laboratory. *Planet. Space Sci.* 59 (11-12), 1114–1127. doi:10.1016/j.pss.2010.06.016

Grotzinger, J. P., Gupta, S., Rubin, D., Schieber, J., Sumner, D. Y., Stack, K. M., et al. (2015). Deposition, exhumation, and paleoclimate of an ancient lake deposit, Gale Crater, Mars. *Science* 350 (6257), aac7575. doi:10.1126/science.aac7575

Gullikson, A. G., Anderson, R. B., and Williams, R. M. E. (2023). Spatial and temporal distribution of sinuous ridges in southeastern Terra Sabaea and the northern region of Hellas Planitia, Mars☆. *Icarus* 394 (14), 115399. doi:10.1016/j.icarus.2022.115399

Gwinner, K., Scholten, F., Preusker, F., Elgner, S., Roatsch, T., Spiegel, M., et al. (2010). Topography of Mars from global mapping by HRSC high-resolution digital terrain

models and orthoimages: Characteristics and performance. *Earth Planet. Sci. Lett.* 294 (3-4), 506–519. doi:10.1016/j.epsl.2009.11.007

Hagar, D. J. (1966). Geomorphology of Coyote Valley, San Bernardino County, California. Ph.D. diss. Amherst, Massachusetts: University of Massachusetts, 210.

Hartmann, W. K. (2005). Martian cratering. 8. Isochron refinement and the history of martian geologic activity. *Icarus* 294, 294–320. doi:10.1016/j.icarus.2004.11.023

Hayden, A. T., and Lamb, M. (2020). Fluvial sinuous ridges of the Morrison Formation, USA: Meandering, scarp retreat, and implications for Mars. *J. Geophys. Res. Planets* 125 (10), e2020JE006470. doi:10.1029/2020JE006470

Hayden, A. T., McElroy, B. J., Lamb, M. P., Williams, R. M. E., Ewing, R. C., and Fischer, W. W. (2019). Formation of sinuous ridges by inversion of river-channel belts in Utah, USA, with implications for Mars. *Icarus* 332 (1), 92–110. doi:10.1016/j.icarus.2019.04.019

Hill, J. R. (2022). Martian chloride salts in the thermal infrared. PhD. Diss. Arizona State University, 365.

Holmes, J. A., and Hoelzmann, P. (2017). "The Late Pleistocene-Holocene African Humid Period as evident in lakes," in *Oxford Encyclopedia of Climate Science*. Oxford: Oxford University Press. doi:10.1093/acrefore/9780190228620.013.531

Hooke, J. M., and Yorke, L. (2011). Channel bar dynamics on multidecadal timescales in an active meandering river. *Earth Surf. Process. Landforms* 36 (14), 1910–1928. doi:10.1002/esp.2214

Howard, A. D., Moore, J. M., and Irwin, R. P., III (2005). An intense terminal epoch of widespread fluvial activity on early Mars: 1. Valley network incision and associated deposits. *J. Geophys. Res. Planets* 110 (E12). doi:10.1029/2005JE002459

Hynek, B. M. (2016). Research focus: the great climate paradox of ancient Mars. *Geology* 44 (10), 879–880. doi:10.1130/focus102016.1

Hynek, B. M., and Di Achille, G. (2017). "Geological map of the Meridiani Planum, Mars," *USGS scientific investigations series (Map 3356, scale 1:2,000,000)*. Reston, VA: U.S. Geological Survey. doi:10.3133/sim3356

Hynek, B. M., Breach, M., and Hoke, M. R. T. (2010). Updated global map of martian valley networks and implications for climate and hydrologic processes. *J. Geophys. Res. Planets* 115, 14. doi:10.1029/2009JE003548

Hynek, B. M., Osterloo, M. K., and Klierein-Young, K. S. (2015). Late-stage formation of martian chloride salts through ponding and evaporation. *Geology* 43 (9), 787–790. doi:10.1130/G36895.1

Irwin, R. P., and Zimbelman, J. R. (2012). Morphometry of Great Basin pluvial shore landforms: implications for paleolake basins on Mars. *J. Geophys. Res. Planets* 117 (E07004), 2012JE004046. doi:10.1029/2012je004046

Irwin, R. P., III, Howard, A. D., Craddock, R. A., and Moore, J. M. (2005). An intense terminal epoch of widespread fluvial activity on early Mars: 2. Increased runoff and Paleolake development. *J. Geophys. Res. Planets* 110, E12S15. doi:10.1029/2005JE002460

Irwin, R. P. I., Lewis, K. W., Howard, A. D., and Grant, J. A. (2015). Paleohydrology of Eberswalde Crater, Mars. *Geomorphol. Binghampt. Geomorphol. Symp. Spec. issue* 240, 83–101. doi:10.1016/j.geomorph.2014.10.012

Kirk, R. L., Mayer, D. P., Fergason, R. L., Redding, B. L., Galuska, D. M., Hare, T. M., et al. (2021). Evaluating stereo digital terrain model quality at Mars rover landing sites with HRSC, CTX, and HiRISE images. *Remote Sens.* 13 (17), 3511. doi:10.3390/rs13173511

Kiss, T., Sipos, G., and Vass, R. (2022). Alluvial ridge development and structure: Case study on the Upper Tisza, Hungary. *Geogr. Pannonica* 26 (3), 230–240. doi:10.5937/gp26-38365

Korus, J. T., and Joeckel, R. M. (2023). Exhumed fluvial landforms reveal evolution of Late Eocene–Pliocene rivers on the Central and Northern Great Plains, USA. *Geosphere* 19 (3), 695–718. doi:10.1130/GES02587.1

Lamb, M. P., McElroy, B. K., Shaw, J., and Mohrig, D. (2010). Linking river-flood dynamics to hyperpycnal-plume deposits: Experiments, theory, and geological implications. *GSA Bull.* 122 (9-10), 1389–1400. doi:10.1130/B30125.1

Lang, S. C., Payenberg, T. H. D., Reilly, M. R. W., Hicks, T., Benson, J., and Kassan, J. (2004). Modern analogues for dryland sandy fluvial-lacustrine deltas and terminal splay reservoirs. *APPEA J.* 44 (1), 329–356. doi:10.1071/AJ03012

Li, Z.-K., Li, S.-H., and Li, Y.-L. (2025). The large distribution of inverted stream channel terrains in the western Qaidam Basin, North Tibetan Plateau, and implications to the fluvial ridges on Mars. *Geomorphology* 473, 109632. doi:10.1016/j.geomorph.2025.109632

Maizels, J. (1990). Raised channel systems as indicators of palaeohydrologic change: A case study from Oman. *Palaeogeogr. Palaeoclimatol. Palaeoecol.* 76, 241–277. doi:10.1016/0031-0182(90)90115-N

Malin, M. C., and Edgett, K. S. (2000). Sedimentary rocks of early Mars. *Science* 290 (5498), 1927–1937. doi:10.1126/science.290.5498.1927

Malin, M. C., and Edgett, K. S. (2001). Mars Global Surveyor Mars Orbiter Camera: Interplanetary cruise through primary mission. *J. Geophys. Res.* 106 (E10), 23429–23570. doi:10.1029/2000JE001455

Malin, M. C., and Edgett, K. S. (2003). Evidence for persistent flow and aqueous sedimentation on early Mars. *Science* 302, 1931–1934. doi:10.1126/science.1090544

Malin, M. C., Bell, J. F., III, Cantor, B. A., Caplinger, M. A., Calvin, W. M., Clancy, R. T., et al. (2007). Context Camera investigation on board the Mars Reconnaissance Orbiter. *J. Geophys. Res.* 112 (E05S04). doi:10.1029/2006JE002808

Mangold, N., Adeli, S., Conway, S., Ansan, V., and Langlais, B. (2012). A chronology of early Mars climatic evolution from impact crater degradation. *J. Geophys. Res.* 117 (E04003). doi:10.1029/2011JE004005

Mangold, N., Williams, R. M. E., and Caravaca, G. (2024). Architecture of the fluvial and deltaic deposits of the east of Jezero crater western fan. *J. Geophys. Res. Planets* 129 (3). doi:10.1029/2023JE008204

Marchetti, D. W., Hynek, S. A., and Cerling, T. E. (2012). Gravel-capped benches above northern tributaries of the Escalante River, South-Central Utah. *Geosphere* 8 (4), 835–853. doi:10.1130/ges00772.1

Mars Channel Working Group (1983). Channels and valleys on Mars. *GSA Bull.* 94 (9), 1035–1054. doi:10.1130/0016-7606(1983)94<1035:cavom>2.0.co;2

Maxwell, T. A., Issawi, B., and Haynes, C. V. (2010). Evidence for Pleistocene lakes in the Tushka region, South Egypt. *Geology* 38, 1135–1138. doi:10.1130/G31320.1

Mayer, D. P. (2018). An improved workflow for producing digital Terrain models of Mars from CTX Stereo data using the NASA Ames Stereo Pipeline, LPSC XLIX, abstract. #1604. Available online at: https://www.hou.usra.edu/meetings/lpsc2018/pdf/1604.pdf (Accessed May 15, 2025).

Mayer, D. P., and Kite, E. S. (2016). An integrated workflow for producing digital terrain models of Mars from CTX and HiRISE stereo data using the NASA Ames Stereo Pipeline, LPSC XLVII, abstract. #1241. Available online at: https://www.hou.usra.edu/meetings/lpsc2016/pdf/1241.pdf (Accessed May 15, 2025).

McEwen, A. S., Eliason, E. M., Bergstrom, J. W., Bridges, N. T., Hansen, C. J., Delamere, W. A., et al. (2007). Mars Reconnaissance Orbiter's High Resolution Imaging Science Experiment (HiRISE). *J. Geophys. Res.* 112 (E05S02), 2005JE002605. doi:10.1029/2005je002605

Meek, N. C. (1994). The stratigraphy and geomorphology of Coyote basin. *San Bernardino Co. Mus. Assoc. Q.* Editor J. Reynolds 41 (3), 5–13.

Menking, K. M., Anderson, R. Y., Shafike, N. G., Syed, K. H., and Allen, B. D. (2004). Wetter or colder during the Last Glacial Maximum? Revisiting the pluvial lake question in southwestern North America. *Quat. Res.* 62, 280–288. doi:10.1016/j.yqres.2004.07.005

Miall, A. D. (1985). Architectural-element analysis: a new method of facies analysis applied to fluvial deposits. *Earth-Science Rev.* 22, 261–308. doi:10.1016/0012-8252(85)90001-7

Miller, D. M., Dudash, S. L., and McGeehin, J. P. (2018). "Paleoclimate record for Lake Coyote, California, and the Last Glacial Maximum and deglacial paleohydrology (25 to 14 cal ka) of the Mojave River," *Saline to freshwater: The diversity of Western Lakes in space and time*. Editors S. W. Starratt, and M. R. Rosen (Boulder: Geological Society of America Special Paper), 536, 201–220. doi:10.1130/2018.2536(12

Moore, J. M. (1990). Nature of the mantling deposit in the heavily cratered terrain of northeastern Arabia, Mars. *J. Geophys. Res. Planets.* 95 (B9), 14279–14289. doi:10.1029/JB095iB09p14279

Moore, J. M., and Howard, A. D. (2005). Large alluvial fans on Mars. *J. Geophys. Res. Planets.* 110, E04005. doi:10.1029/2004JE002352

Moore, J. M., Howard, A. D., Dietrich, W. E., and Schenk, P. M. (2003). Martian layered fluvial deposits: implications for Noachian climate scenarios. *Geophys. Res. Lett.* 30 (24), 2003GL019002. doi:10.1029/2003GL019002

Morgan, A. M., Howard, A. D., Hobley, D. E., Moore, J. M., Dietrich, W. E., Williams, R. M. E., et al. (2014). Sedimentology and climatic environment of alluvial fans in the martian Saheki crater and a comparison with terrestrial fans in the Atacama Desert. *Icarus* 229, 131–156. doi:10.1016/j.icarus.2013.11.007

Morgan, A. M., Wilson, S. A., and Howard, A. D. (2022). The global distribution and morphologic characteristics of fan-shaped sedimentary landforms on Mars. *Icarus* 385, 115137. doi:10.1016/j.icarus.2022.115137

Morrison, R. B. (1991). "Chapter 10: Quaternary stratigraphic, hydrologic, and climatic history of the Great Basin, with emphasis on Lakes Lahontan, Bonneville, and Tecopa," in *Quaternary nonglacial geology: Conterminous U. S., the geology of North America*. Editor R. B. Morrison (Boulder, CO: Geological Society of America), K-2, 283–320. doi:10.1130/DNAG-GNA-K2.283

Neukum, G., Jaumann, R., and HRSC Team (2004). "HRSC: The High Resolution Stereo Camera of Mars Express," in *Mars Express: the scientific payload*. Noordwijk, Netherlands: European Space Agency. Editor A. Wilson, 17–35.

Newsom, H. E., Brittelle, G. E., Hibbitts, C. A., Crossey, L. J., and Kudo, A. M. (1996). Impact crater lakes on Mars. *J. Geophys. Res.* 101 (E6), 14951–14955. doi:10.1029/96JE01139

Nicholas, A., Aalto, R., Sambrook Smith, G., and Schwendel, A. (2018). Hydrodynamic controls on alluvial ridge construction and avulsion likelihood in meandering river floodplains. *Geology* 46 (7), 639–642. doi:10.1130/G40104.1

Osterloo, M. M., Hamilton, V. E., Bandfield, J. L., Glotch, T. D., Baldridge, A. M., Christensen, P. R., et al. (2008). Chloride-bearing materials in the

southern highlands of Mars. *Science* 319, 1651–1654. doi:10.1126/science.1150690

Osterloo, M. M., Anderson, F. S., Hamilton, V. E., and Hynek, B. M. (2010). Geologic context of proposed chloride-bearing materials on Mars. *J. Geophys. Res.* 115 (E10012). doi:10.1029/2010JE003613

Oviatt, C. G. (1997). Lake Bonneville fluctuations and global climate change. *Geology* 25 (2), 155–158. doi:10.1130/0091-7613(1997)025<0155:lbfagc>2.3.co;2

Oviatt, C. G., Madsen, D. B., and Schmitt, D. N. (2003). Late Pleistocene and Early Holocene rivers and wetlands in the Bonneville basin of Western North America. *Quat. Res.* 60, 200–210. doi:10.1016/S0033-5894(03)00084-X

Pain, C. F., and Ollier, C. D. (1995). Inversion of relief–a component of landscape evolution. *Geomorphology* 12, 151–165. doi:10.1016/0169-555X(94)00084-5

Pain, C. F., Clarke, J. D. A., and Thomas, M. (2007). Inversion of relief on Mars. *Icarus* 190 (2), 478–491. doi:10.1016/j.icarus.2007.03.017

Palucis, M., Dietrich, W. E., Williams, R. M. E., Hayes, A. G., Parker, T., Sumner, D. Y., et al. (2016). Sequence and relative timing of large lakes in Gale Crater (Mars) after the formation of Mt. Sharp. *J. Geophys. Res. Planets* 121, 25. doi:10.1016/10.1002/2015JE004905

Placzek, C., Quade, J., and Patchett, P. J. (2006). Geochronology and stratigraphy of Late Pleistocene lake cycles on the Southern Bolivian Altiplano: Implications for causes of tropical climate change. *GSA Bull.* 118, 515–532. doi:10.1130/B25770.1

Reheis, M. C. (1999). *Extent of Pleistocene Lakes in the Western Great Basin: USGS miscellaneous field studies map MF-2323*. Denver, CO: U.S. Geological Survey. Available online at: http://pubs.usgs.gov/mf/1999/mf-2323.

Reheis, M. C., Miller, D. M., McGeehin, J. P., Redwine, J. R., Oviatt, C. G., and Bright, J. E. (2015). Directly dated MIS 3 lake-level record from Lake Manix, Mojave Desert, California, USA. *Quat. Res.* 83 (1), 187–203. doi:10.1016/j.yqres.2014.11.003

Ribó, M., Mountjoy, J., Mitchell, N. C., Watson, S. J., Hoffmann, J. J. L., and Woelz, S. (2024). New insights on gravity flow dynamics during submarine canyon flushing events. *Geology* 53, 34–39. doi:10.1130/G52424.1

Russell, I. C. (1885). *Geological history of Lake Lahontan, a Quaternary lake of northwestern Nevada. Monograph 11*. Washington, DC: United States Geological Survey, 288. doi:10.3133/m11

Sagan, C., Toon, O. B., and Gierasch, P. J. (1973). Climatic change on Mars. *Science* 181, 1045–1049. doi:10.1126/science.181.4104.1045

Schieber, J. M., Minitti, M. E., Sullivan, R., Edgett, K. S., Malin, M. C., Parker, T. J., et al. (2020). Engraved on the rocks—Aeolian abrasion of martian mudstone exposures and their relationship to modern wind patterns in Gale Crater, Mars. *Depositional Rec.* 6, 625–647. doi:10.1002/dep2.110

Schieber, J., Bohacs, K. M., Bish, D., Coleman, M., Thompson, L., Rapin, W., et al. (2024). Evaporitic–lacustrine mudstone laminites and prodelta mudlobes – continuity and change in the Hartmann's Valley interval, Murray Formation, Gale Crater, Mars. *Sedimentology* 71 (7), 2071–2118. doi:10.1111/sed.13242

Schon, S. C., Head, J. W., III, and Fassett, C. I. (2012). An overfilled lacustrine system and progradational delta in Jezero Crater, Mars: Implications for Noachian climate. *Planet. Space Sci.* 67 (1), 28–45. doi:10.1016/j.pss.2012.02.003

Slingerland, R., and Smith, N. D. (1998). Necessary conditions for a meandering-river avulsion. *Geology* 26 (5), 435–438. doi:10.1130/0091-7613(1998)026<0435:ncfamr>2.3.co;2

Stucky de Quay, G., Goudge, T., Kite, E., Fassett, C., and Guzewich, S. (2021). Limits on runoff episode duration for early Mars: Integrating lake hydrology and climate models. *Geophys. Res. Lett.* 48 (15), e2021GL093523. doi:10.1029/2021GL093523

Swartz, J. M., Cardenas, B. T., Mohrig, D., and Passalacqua, P. (2022). Tributary channel networks formed by depositional processes. *Nat. Geosci.* 15 (3), 216–221. doi:10.1038/s41561-022-00900-x

Talling, P. J., Wynn, R. B., Schmmidt, D. N., Rixon, R., Sumner, E., and Amy;, L. (2010). How did thin submarine debris flows carry boulder-sized intraclasts for remarkable distances across low gradients to the far reaches of the Mississippi fan? *J. Sediment. Res.* 80 (10), 829–851. doi:10.2110/jsr.2010.076

Vanden Berg, M. (2019). Domes, rings, ridges, and polygons: Characteristics of microbialites from Utah's Great Salt Lake. *Sediment. Rec.* 17 (1), 4–10. doi:10.2110/sedred.2019.1.4

Wells, S. G., Brown, W. J., Enzel, Y., Anderson, R. Y., and McFadden, L. D. (2003). "Late Quaternary geology and paleohydrology of pluvial Lake Mojave, Southern California," *Paleoenvironments and paleohydrology of the Mojave and southern Great Basin deserts*. Editors Y. Enzel, S. G. Wells, and N. Lancaster (Boulder: Geological Society of America Special), 368, 79–114. doi:10.1130/0-8137-2368-X.79

Williams, R. M. E., and Weitz, C. M. (2014). Reconstructing the aqueous history within the southwestern Melas basin, Mars: Clues from stratigraphic and morphometric analyses of fans. *Icarus* 242, 19–37. doi:10.1016/j.icarus.2014.06.030

Williams, R. M. E., Chidsey, T. C., and Eby, D. E. (2007). "Exhumed paleochannels in central Utah - analogs for raised curvilinear features on Mars," in *Central Utah - diverse geology of a dynamic landscape*. Editors G. C. Willis, M. E. Hylland, D. L. Clark, and T. C. Chidsey (Salt Lake City, Utah: Utah Geological Association), 220–235. Publication 36.

Williams, R. M. E., Irwin, R. P. I. I. I., and Zimbelman, J. R. (2009). Evaluation of paleohydrologic models for terrestrial inverted channels: Implications for application to martian sinuous ridges. *Geomorphology* 107, 300–315. doi:10.1016/j.geomorph.2008.12.015

Williams, R. M. E., Rogers, A. D., Chojnacki, M., Boyce, J., Seelos, K. D., Hardgrove, C., et al. (2011). Evidence for episodic alluvial fan formation in far western Terra Tyrrhena, Mars. *Icarus* 211 (1), 222–237. doi:10.1016/j.icarus.2010.10.001

Williams, R. M. E., Irwin, R. P., III, Zimbelman, J. R., Chidsey, T. C., Jr., and Eby, D. E. (2011). "Field guide to exhumed paleochannels near Green River, Utah: Terrestrial analogs for sinuous ridges on Mars," *Analogs for planetary exploration*. Editors W. B. Garry, and J. E. Bleacher (Geological Society of America Special Paper), 483, 483–505. doi:10.1130/2011.2483(29

Williams, R. M. E., Irwin, R. P. I., Burr, D. M., Harrison, T., and McClelland, P. (2013). Variability in martian sinuous ridge form: Case study of Aeolis Serpens in the Aeolis Dorsa, Mars, and insight from the Mirackina paleoriver, South Australia. *Icarus* 225 (1), 308–324. doi:10.1016/j.icarus.2013.03.016

Williams, R. M. E., Noe Dobrea, E. Z., Irwin, R. P., III, Howard, A. D., Dietrich, W. D., and Crawley, J. C. (2021). Inverted channel variations identified on a distal portion of a bajada in the Central Atacama Desert, Chile. *Geomorphology* 393, 107925. doi:10.1016/j.geomorph.2021.107925

Williams, R. M. E., Caravaca, G., Gupta, S., Horgan, B., Hurowitz, J., Ives, L. R. W., et al. (2023). Investigation of sedimentary fan deposits along the Beagle Gap traverse at Jezero Crater, Mars, GSA fall meeting. *Geol. Soc. Am. Abstr. Programs* 55 (6), 393229. Abstract # 393229. doi:10.1130/abs/2023AM-393229

Williams, R. M. E., Anderson, R. B., Gullikson, A. L., and Berman, D. C. (2024). Digital terrain models for Mars sinuous ridges and alluvial fans projects: U.S. Geological Survey data release. Available online at: https://doi.org/10.5066/P9I1QO1U (Accessed July 23, 2024).

Wilson, S. A., Howard, A. D., Moore, J. M., and Grant, J. A. (2007). Geomorphic and stratigraphic analysis of Crater Terby and layered deposits north of Hellas Basin, Mars. *J. Geophys. Res. Planets* 112 (E08009). doi:10.1029/2006JE002830

Wilson, S. A., Morgan, A. M., Howard, A. D., and Grant, J. A. (2021). The global distribution of craters with alluvial fans and deltas on Mars. *Geophys. Res. Lett.* 48 (4), e2020GL091653. doi:10.1029/2020GL091653

Yang, X., and Scuderi, L. A. (2017). Hydrological and climatic changes in deserts of China since the Late Pleistocene. *Quat. Res.* 73 (1), 1–9. doi:10.1016/j.yqres.2009.10.011

Zabrusky, K., Andrews-Hanna, J. C., and Wiseman, S. M. (2012). Reconstructing the distribution and depositional history of the sedimentary deposits of Arabia Terra, Mars. *Icarus* 220 (2), 311–330. doi:10.1016/j.icarus.2012.05.007

Zaki, A. S., Gigengack, R., and Castelltort, S. (2020). "Inverted channels in the Eastern Sahara—distribution, formation, and interpretation to enable reconstruction of paleodrainage networks," in *Paleohydrology*. Editors J. Herget, and A. Fontana (Springer Nature Switzerland), 117–13. doi:10.1007/978-3-030-23315-0_6

Zaki, A. S., Pain, C. F., Edgett, K. S., and Castelltort, S. (2021). Global inventory of fluvial ridges on Earth and lessons applicable to Mars. *Earth-Science Rev.* 216 (1036561), 103561. doi:10.1016/j.earscirev.2021.103561

Zhao, J., Wang, J., Zhang, M., and Xiao, L. (2021). Unique curvilinear ridges in the Qaidam Basin, NW China: Implications for martian fluvial ridges. *Geomorphology* 372 (5), 107472. doi:10.1016/j.geomorph.2020.107472

Zuber, M. T., Smith, D. E., Solomon, S. C., Muhleman, D. O., Head, J. W., Garvin, J. B., et al. (1992). The Mars Observer Laser Altimeter investigation. *J. Geophys. Res. Planets* 97, 7781–7797. doi:10.1029/92JE00341